

CHARACTERIZATION OF
SEISMIC AMPLITUDE ANOMALIES AT HIBERNIA
USING 3D SEISMIC DATA

Bill Phu

Submitted in Partial Fulfillment of the Requirements
for the degree of Bachelor of Science
Dalhousie University, Halifax, Nova Scotia.
April, 1998.

Distribution License

DalSpace requires agreement to this non-exclusive distribution license before your item can appear on DalSpace.

NON-EXCLUSIVE DISTRIBUTION LICENSE

You (the author(s) or copyright owner) grant to Dalhousie University the non-exclusive right to reproduce and distribute your submission worldwide in any medium.

You agree that Dalhousie University may, without changing the content, reformat the submission for the purpose of preservation.

You also agree that Dalhousie University may keep more than one copy of this submission for purposes of security, back-up and preservation.

You agree that the submission is your original work, and that you have the right to grant the rights contained in this license. You also agree that your submission does not, to the best of your knowledge, infringe upon anyone's copyright.

If the submission contains material for which you do not hold copyright, you agree that you have obtained the unrestricted permission of the copyright owner to grant Dalhousie University the rights required by this license, and that such third-party owned material is clearly identified and acknowledged within the text or content of the submission.

If the submission is based upon work that has been sponsored or supported by an agency or organization other than Dalhousie University, you assert that you have fulfilled any right of review or other obligations required by such contract or agreement.

Dalhousie University will clearly identify your name(s) as the author(s) or owner(s) of the submission, and will not make any alteration to the content of the files that you have submitted.

If you have questions regarding this license please contact the repository manager at dalspace@dal.ca.

Grant the distribution license by signing and dating below.

Name of signatory

Date

Abstract

The Chevron et al. Hibernia P-15 well penetrated one of many bright spots and encountered gas. Bright spots are one of four 'direct hydrocarbon indicators' and result from the high acoustic impedance contrast from gas accumulations in Tertiary sediments. Many of these bright spots occur at or near the same stratigraphic level in the South Mara Unit, which is bounded by two main unconformity reflections: the Base Tertiary Unconformity and another regionally extensive unnamed one overlying the South Mara Unit. Paleo-environmental interpretation using seismic and well log data suggests that the P-15 well penetrated a near shore sand body that was preserved during a transgression. The transgression was marked by localized erosion so many other sand units are not preserved. Other bright spots in the South Mara may be the result of tuning effects and may or may not contain any dissolved gas.

Key Words: Bright spots, Direct Hydrocarbon Indicators, Shallow Gas, Jeanne d'Arc Basin

Table of Contents

1	INTRODUCTION	1
1.1	Purpose and Scope.....	1
1.2	Geologic Background.....	7
1.2.1	Physiography of the Grand Banks	7
1.2.2	Evolution of the Jeanne d’Arc Basin	8
2	STUDY INTERVAL.....	11
2.1	South Mara Unit Sequence Stratigraphy	11
2.2	Hydrocarbon Potential.....	12
2.3	Geophysical Data.....	17
3	THEORETICAL BACKGROUND	19
3.1	Reflection Seismology.....	19
3.2	2D vs 3D Seismic Data.....	25
3.3	Seismic Stratigraphy.....	29
3.4	Direct Hydrocarbon Indicators	33
3.4.1	Other Causes of Amplitude Anomalies	37
3.4.2	Tuning Effects.....	37
3.5	Well Information	38
3.5.1	Gamma Ray Log.....	38
3.5.2	Sonic Log.....	40
3.6	Trap Types.....	40
3.7	Software and Hardware	42
4	SEISMIC INTERPRETATION	45
4.1	Work Flow.....	45
4.2	Mapped Horizons	45
4.3	South Mara Unit Stratigraphic Interpretation.....	47
4.4	Gas Trapping Mechanism.....	47
4.5	Direct Hydrocarbon Indicators	48
5	DISCUSSION.....	61
6	CONCLUSIONS.....	67
7	REFERENCES AND BIBLIOGRAPHY	69

Table of Figures

Figure 1.1 The Hibernia P-15 well penetrating a bright spot. This bright spot has been correlated with gas. Seismic section A-A'. See Figure 2.5 for section location.	2
Figure 1.2 Bright spot at Hibernia that has been correlated with gas. Seismic section B-B' See Figure 2.5 for location.	3
Figure 1.3 Location map showing the location of the Hibernia field and the five interconnected Mesozoic Basins.	4
Figure 1.4 Tectonic and structural elements of the Jeanne d'Arc.	5
Figure 1.5 Generalized Mesozoic and Tertiary stratigraphic column of the Jeanne d'Arc Basin.	6
Figure 2.1 Friis (1997) summary stratigraphic column and sequences for the South Mara Unit.	14
Figure 2.2 Gamma Ray, Sonic and Lithologic data from Hibernia P-15.	15
Figure 2.3 Sinclair et al. (1992) schematic diagram showing the shale bounded sandstone stratigraphic group of plays.	16
Figure 2.1 map showing 3D survey and wells (from Friis, 1997).	18
Figure 3.1 Partitioning of amplitude at an interface.	23
Figure 3.1 Schematic diagram of the Fresnel zone and how it is affected by migration (2D and 3D cases).	27
Figure 3.2 Stratal geometric relationships at sequence boundaries.	28
Figure 3.1 Relative acoustic impedance conditions required to produce various DHI's	35
Figure 3.2 Seismic model of tuning occurring at a sand wedge pinchout. This diagram shows the relationship between dominant seismic wavelength and bed thickness. A basic 25 Hz Ricker wavelet is used in the model. From Robertson and Nogami (1984).	36
Figure 3.3 Tuning curves for two zero phase wavelets. There is a dependence on the wavelet used, but below the tuning thickness, the amplitude changes considerably while apparent thickness does not change appreciably.	36
Figure 3.1 Some possible structural traps.	44
Figure 3.2 Some sample stratigraphic traps.	44
Figure 4.1 E-W seismic profile illustrating the two main reflection surfaces interpreted.	51
Figure 4.2 N-S seismic profile showing the two principal reflections interpreted. ...	52

Figure 4.1 E-W seismic profile illustrating the two main reflection surfaces interpreted.....	51
Figure 4.2 N-S seismic profile showing the two principal reflections interpreted. ...	52
Figure 4.3 Map and 3D perspective view of the BTU reflection.....	53
Figure 4.4 Seismic section showing local reduction in amplitude of the BTU reflection.	54
Figure 4.5 Horizon amplitude extraction of the BTU reflection.	55
Figure 4.6 Map and 3D perspective view of the UA reflection.....	56
Figure 4.7 E-W image of the bright spot near B-27 which seems to indicate paleo-geomorphology.	57
Figure 4.8 N-S image of bright spot near B-27 which may indicate that the bright spot is a paleo-geomorphologic feature, possibly a sediment fan.....	58
Figure 4.9 A shaded relief map of the BTU reflection with highly negative amplitudes highlighted in red.....	59
Figure 4.10 A close up of the bright spots near P-15 and B-27. Compare this to other amplitude anomalies which may be a result of tuning.	60
Figure 5.1 Change in relative sea level and geometry of sand bars that may result. From Moslow (1984).	64
Figure 5.2 Iron geochemistry diagram to relate iron minerals to environment. From Boggs (1995).....	65

Table of Tables

Table 3.1 Mechanisms for energy loss	24
Table 3.2 Seismic characteristics and Environmental Facies Interpretation of Clastic Facies Units.....	31
Table 5.1 Sandstone reservoir characteristics for the principal depositional environments.....	65

Acknowledgements

I would like to thank the Geological Survey of Canada (Atlantic) for very kindly permitting me to use their resources to complete this project. Also, I thank my classmates for lending a sympathetic ear through the trials and tribulations of the last few months. Lastly, I cannot thank Ellen Johnson enough for her support and persistence in getting me to finish this.

Abbreviations

2D	Two-dimensional seismic data
3D	Three-dimensional seismic data
BTU	Base Tertiary Unconformity
CNOPB	Canada-Newfoundland Offshore Petroleum Board
DHI	Direct Hydrocarbon Indicators
DSDP	Deep Sea Drilling Project
DST	Drill Stem Test
GSC-A	Geological Survey of Canada (Atlantic)
HST	High-stand systems tract
Mmcf/d	Measure of gas production (Millions of cubic feet per day)
ODP	Ocean Drilling Project
SGI	Silicon Graphics, Inc.
TST	Transgressive Systems Tract
TWT	Two Way Travel time
UA	Unconformity 'A'
[]	Dimensional units, where
	M is Mass
	L is Length
	T is Time

1 INTRODUCTION

High amplitude reflections (bright spots) at shallow depth are a prominent feature of seismic profiles at the Hibernia giant oilfield, offshore Newfoundland (Figure 1.1 and Figure 1.2). The Hibernia discovery well, Chevron et al. Hibernia P-15, penetrated one of these seismic bright spots and encountered dissolved gas in 1979. When this interval was tested, it only produced water and mud. Although no commercial quantities of gas were discovered at Hibernia, bright spots have been correlated with gas occurrences here and in many other oil provinces of the world.

1.1 Purpose and Scope

The purpose of this project is to answer the question: *why are these bright spots there?* Amplitude anomalies such as bright spots occur as a result of several processes. They are usually indicative of some gas accumulation, and occasionally other natural phenomena. This study will focus on the bright spots which are caused by dissolved gas. Sometimes, the mechanism creating bright spots are not always obvious. Characterizing where and how these bright spots occur may differentiate between gas accumulations and other effects.

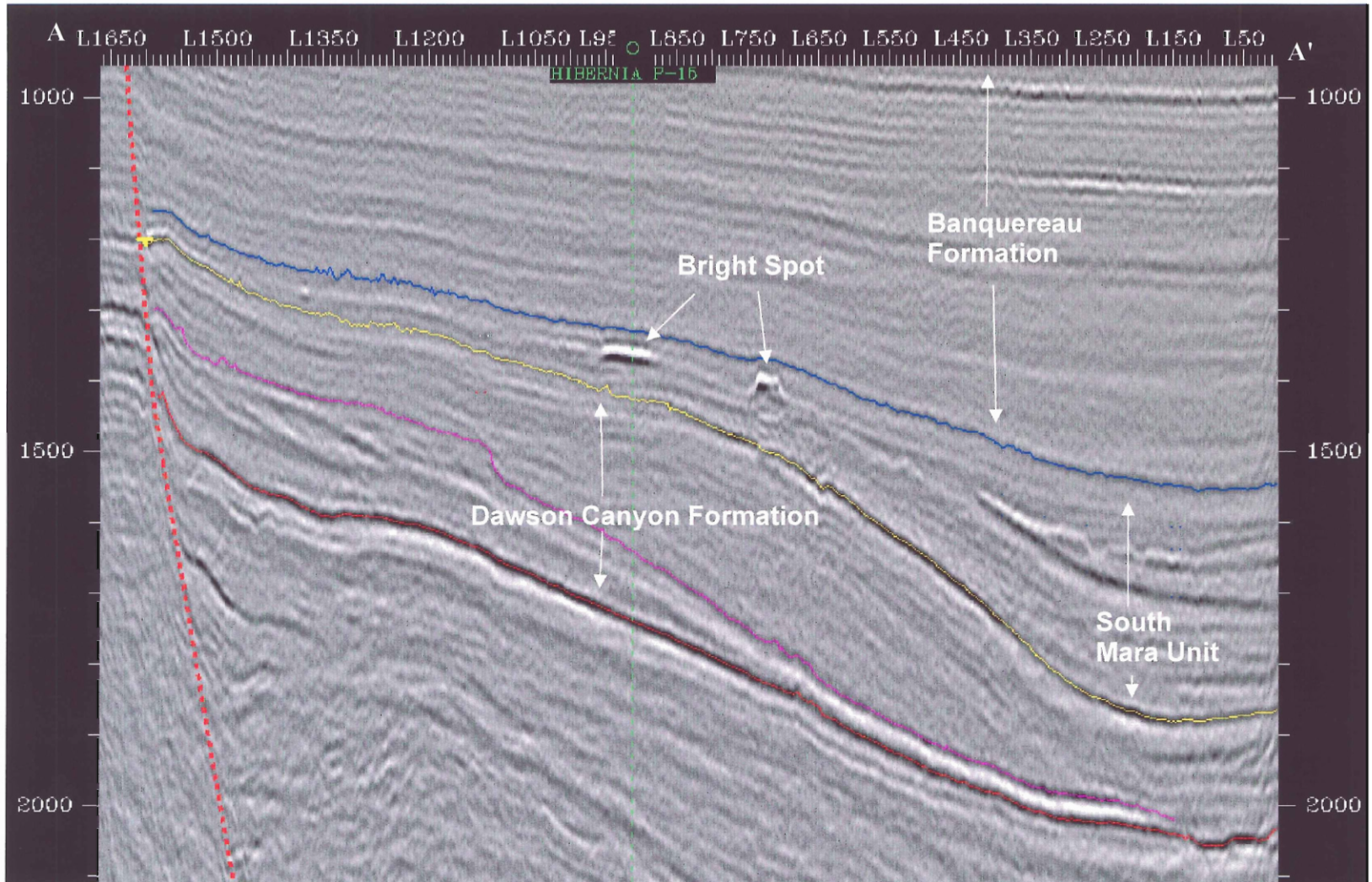


FIGURE 1.1 Seismic section A-A' at Hibernia, showing two bright spots, including one generated by the Chevron et al. Hibernia P-15 well. See Figure 2.5 for location. (Trace 928 of Hibernia 3D survey.)

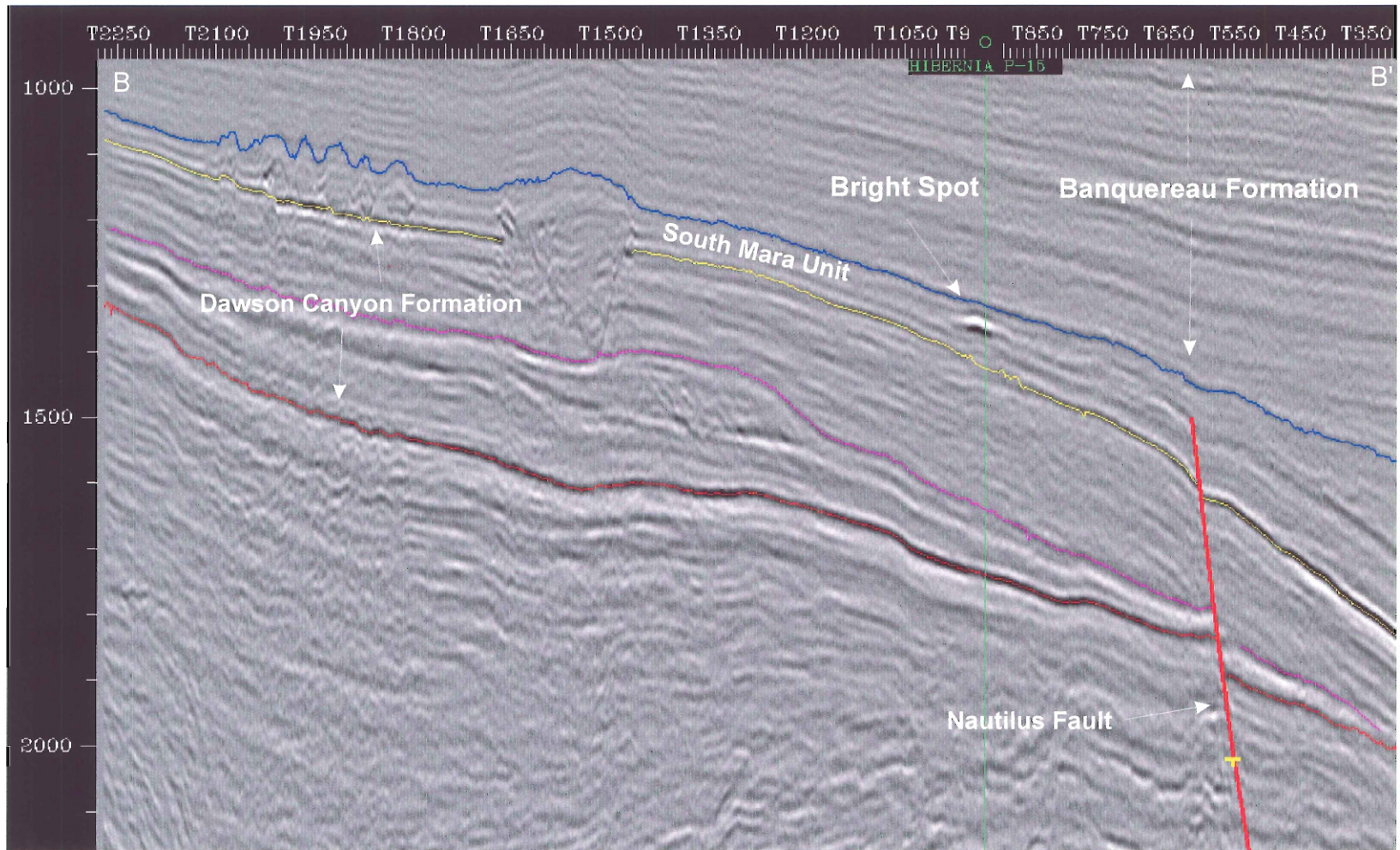


FIGURE 1.2 Seismic section B-B' at Hibernia, showing the bright spot associated with the P-15 well.. See Figure 2.5 for location. (Line 912 of Hibernia 3D survey.)

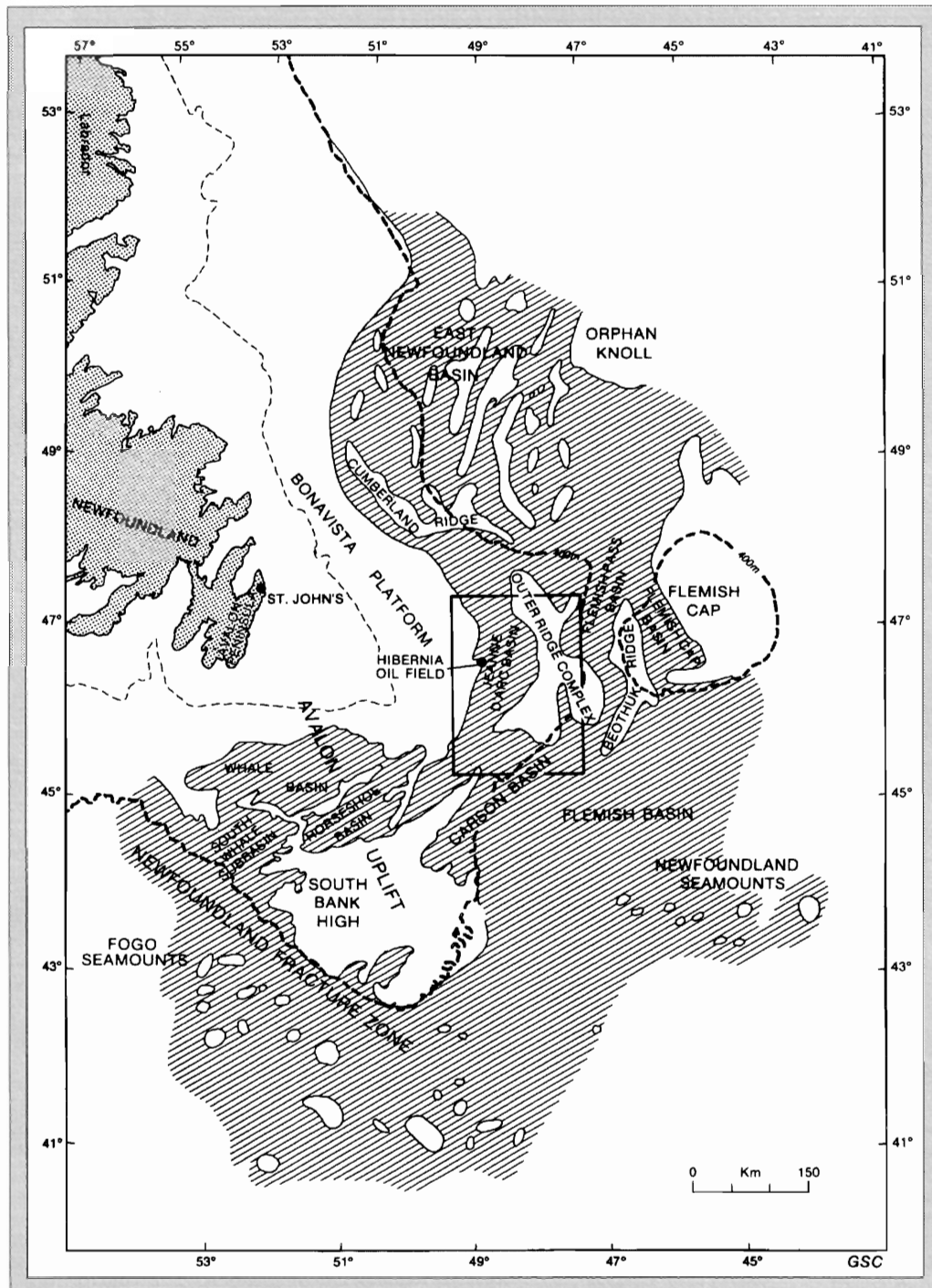


Figure 1.3 Location map showing the location of the Hibernia field and the five interconnected Mesozoic Basins. The box defines the area shown in Figure 1.4. (After Sinclair et al., 1992).

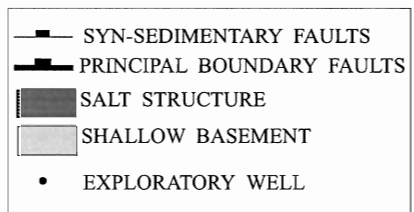
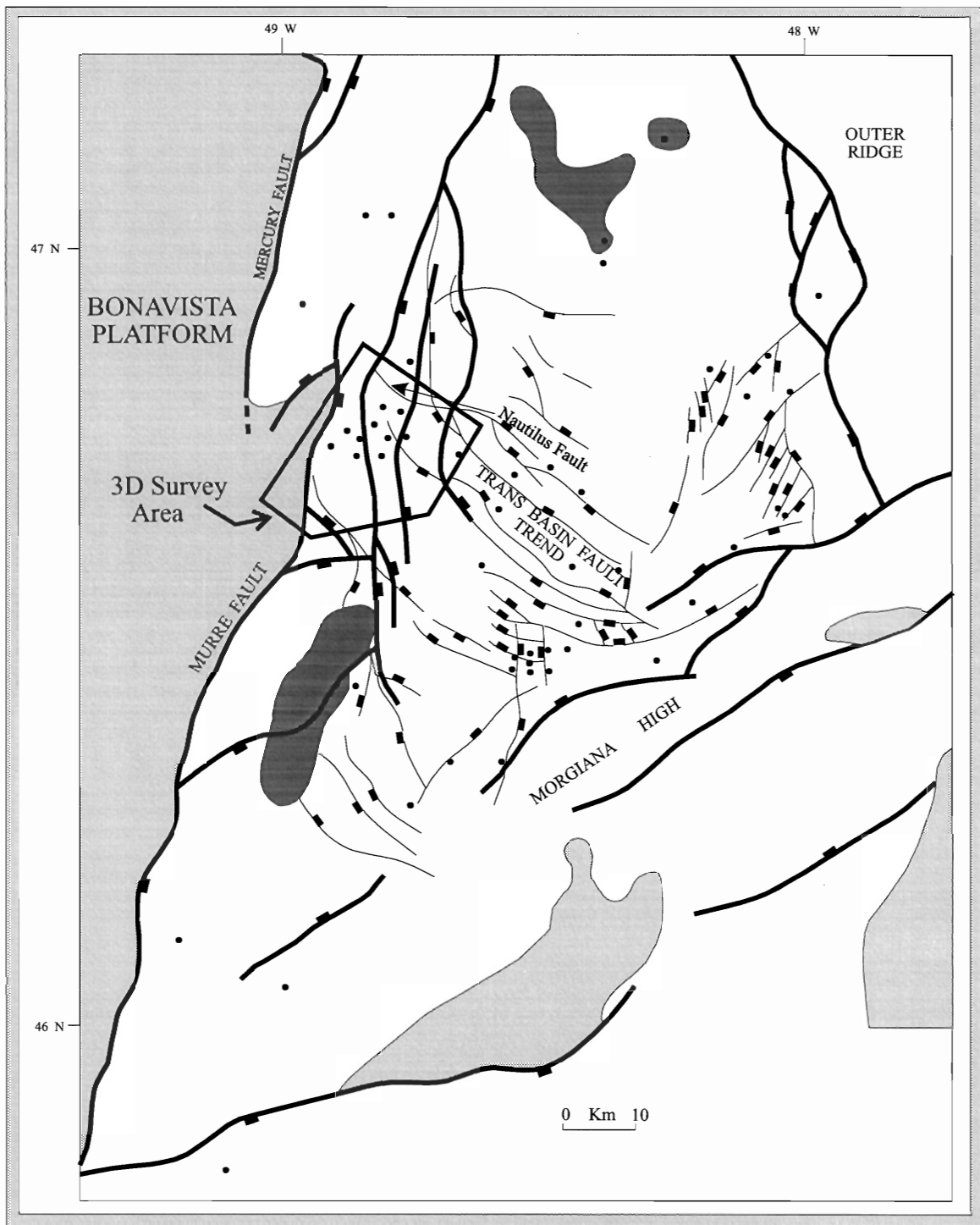


Figure 1.4 Structural elements map of the Jeanne d'Arc Basin. Note the Bonavista Platform to the West and the Outer Ridge Complex to the East. The 3D survey is shown. Note the Trans-Basin Fault Trend. The main fault affecting the sediments of interest is the Nautilus Fault. Modified after Friis (1997).

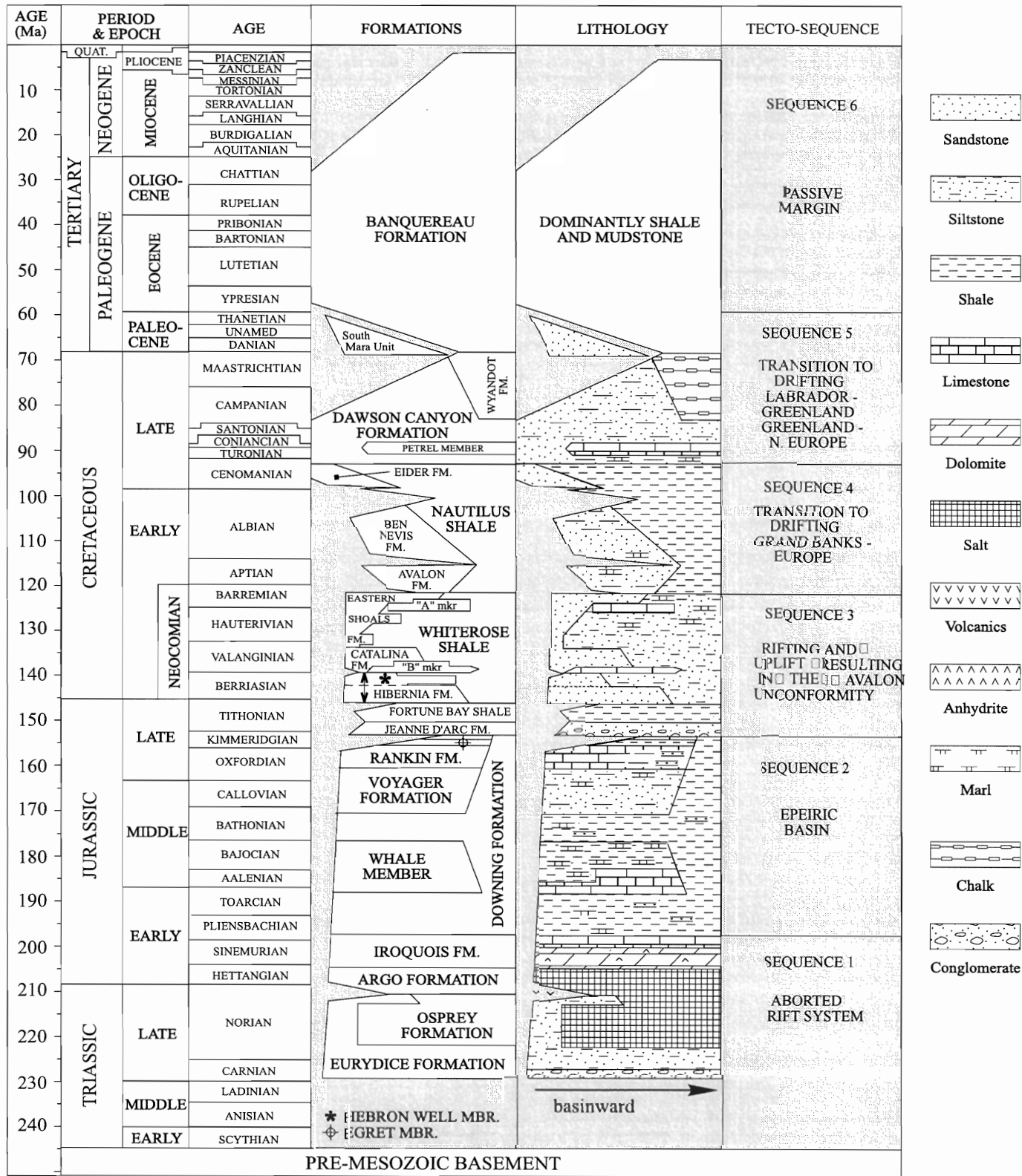


Figure 1.5 Generalized Mesozoic and Tertiary Stratigraphic Column of the Jeanne d'Arc Basin. Included are major sequences defined by McAlpine (1990). From McAlpine (1990).

1.2 Geologic Background

The Hibernia oilfield is located about 350 km southeast of St. John's, Newfoundland, on the Northeastern part of the Grand Banks. This section provides a brief overview of known stratigraphy, and structural and sedimentation history of the Grand Banks and the Jeanne d'Arc.

1.2.1 Physiography of the Grand Banks

Rifting of Pangea during the Mesozoic produced a series of sedimentary basins along the eastern edge of North America. In Canada, these basins stretch from the Fundy Basin to a series of basins on the Grand Banks, and up to Labrador (Wade et al., 1996). Although all of these basins contain thick Mesozoic sediments, commercial hydrocarbons have only been found in two areas: the Jeanne d'Arc Basin underlying the Grand Banks, and the Sable Island area, offshore Nova Scotia.

The Grand Banks of Newfoundland overlie a series of interconnected basins: the South Whale, Whale, Horseshoe, Carson and Jeanne d'Arc Basins (Figure 1.3). The Jeanne d'Arc Basin, a fault bounded half-graben, is the deepest of these basins and contains some 20 km of sediment and thus contains the most complete record of Grand Banks history (McAlpine, 1990; Sinclair et al., 1992). Within the basin is a prominent trans-basin fault trend (Figure 1.4). These faults are mainly associated with rifting during the Triassic and Jurassic. Within the

Hibernia field, the Murre and Nautilus Faults are the only major faults affecting Tertiary sediments.

1.2.2 Evolution of the Jeanne d'Arc Basin

The tectonic and stratigraphic evolution of the Grand Banks resulted from a number of rifting events beginning in the late Triassic and culminating in the Cenomanian. The basement rocks underlying the Jeanne d'Arc Basin consist of late Paleozoic rocks metamorphosed during the Appalachian Orogeny (Sinclair et al., 1992).

During the late Triassic to Early Jurassic, a spreading sea floor propagated from south to north near what is now the eastern limits of North America from Florida to near the Grand Banks. While this period of rifting failed to produce an open ocean, it decoupled North America from Africa. In addition, thick sequences of continental and marine sediments were deposited during the early and mid Jurassic (McAlpine, 1990).

Limited marine magnetic anomaly data and DSDP/ODP drilling results indicate that seafloor spreading between the central Grand Banks and Iberia began in early Aptian time, while farther north, between Flemish Cap and Goban Spur, spreading began by at least late Albian time (Driscoll et al., 1995). Rifting of the Grand Banks was initiated by block motion in either the Kimmeridgian (Grant et al., 1986) or Callovian (Tankard and Welsink, 1988). This second phase of rifting, called the Iberia-Labrador rift, caused the separation of North America, Europe and Greenland (Driscoll et al., 1995; McAlpine, 1990; Sinclair et al.,

1992). Rifting was complete by Paleocene time (Grant et al., 1986). Transform motion along the Newfoundland Fracture Zone, which forms the southern boundary of the Grand Banks, accommodated the extension (Desroches, 1992).

During this stage of tectonic activity, a regional uplift (the Avalon Uplift) produced a peneplain called the Avalon Unconformity which preceded rifting of the Grand Banks, which occurred during Kimmeridgian-Callovian time. The rate of uplift outpaced the rate of trough development and thick fluvial and paralic sequences infilled the developing basins of the incipient Atlantic Ocean (McAlpine, 1990; Sinclair et al., 1992). Due to tectonic overprinting of faults, their timing and orientation, the Jeanne d'Arc basin became asymmetric; the sediments varied from about 4 km thick in the south, to over 20 km thick to the north (McAlpine, 1990). Following this second period of rifting, the Grand Banks began a transition to a passive margin until about Paleocene time. Sediment supply became intermittent and slowly decreased through to the Tertiary.

During the Cenomanian, relative sea level rise inundated the basin margins, leading to the deposition of predominantly shales, marlstones and siltstones (Boyd, 1997). Beginning in the Turonian, two consecutive highstand systems deposited the Dawson Canyon Formation. The first highstand deposited the prograding Otter Bay Unit and the neritic chalky Petrel Member (Friis, 1997; Boyd, 1997). The second highstand deposited the chalk and marlstone Wyandot Member and the deltaic Fox Harbour Member. Both of these submarine fans

were deposited at the base of the shelf and spread eastward as both sea level and accommodation space decreased (Boyd, 1997).

As sea level decreased further, the relative lowstand resulted in the shelf undergoing subaerial exposure and erosion at the beginning of the Tertiary; this is the Base Tertiary Unconformity. Overlying the Base Tertiary Unconformity is the South Mara Unit, which consists predominantly of delta front sands and turbidites (McAlpine, 1990). The shales and siltstones of the Banquereau Formation cap these sediments.

Since the beginning of the Tertiary, changes in sea level may have subjected the Grand Banks to subaerial conditions at least once (McAlpine, 1990). At present, subsidence is probably a result of thermal subsidence and compaction with comparatively low sediment influx.

2 STUDY INTERVAL

Since this study focuses on bright spots located in the South Mara Unit, some detailed background is presented here. This unit has been interpreted to be stratigraphically above the Dawson Canyon Formation and below the Banquereau Formation. Other than this general definition, there is a lack of consensus on what actually constitutes the South Mara Unit. The Canada-Newfoundland Offshore Petroleum Board considers the South Mara to be a *member* of the Banquereau Formation, whereas others consider it to be a distinct unit. The convention used by Friis (1997) and others, that the South Mara is a *unit*, will be used.

2.1 South Mara Unit Sequence Stratigraphy

McAlpine(1990), Friis (1997), M. Deptuck (pers. comm, 1998) and others described the South Mara Unit as an unconformity bounded sequence of sediments. Desilva (1993) interpreted it to be non-conformable near the basin margins and conformable elsewhere in the basin. However, the seismic data used in this study (see section 2.2) cover only a small part of the Jeanne d’Arc basin and the unit is considered to be unconformity bounded within the study area (Friis, 1997).

The South Mara Unit has been interpreted to represent a sediment fan (Sinclair et al., 1992), possibly turbidite deposits (McAlpine, 1990). The South Mara Unit is generally thin within the 3D survey area and thickens northward and towards the center of the Jeanne d'Arc Basin (Figure 1.4).

Workers such as De Silva (1993), Agrawal et al. (1995), Friis (1997) and Deptuck (in progress, 1998) have correlated, mapped and conducted sequence stratigraphic analysis in the Late Cretaceous to Eocene interval. Most workers have used a 2km x 2km 2D seismic grid, while others (Shimeld, pers. comm; Friis, 1997) have made extensive use of the same 3D survey used in this study. Friis (1997) has subdivided the study interval into 6 sequences, 3 of which are in the South Mara Unit.

South Mara lithostratigraphy is predominantly siliciclastic with occasional carbonate cementation. Figure 2.1 summarizes lithostratigraphic zonation of the South Mara within the seismic survey area (Friis, 1997). In the study interval, sand units are generally thin and occur at the base of the South Mara. Sinclair et al. (1992) indicated that the South Mara is extremely variable and that good sand development will be localized.

2.2 Hydrocarbon Potential

Chevron et al. tested the South Mara Unit when they drilled the Hibernia discovery well in 1979. During drilling, gas logs indicated plentiful dissolved gas, with values ranging about 50 ppm dissolved gas. Along a section that

coincides with the seismic bright spot (Figure 2.2) the gas log indicates up to 1-2% dissolved gas. Although it was the first porous zone to be reached, it was not tested until much later. DST #12 finally tested it, but results produced only mud and water. It is possible that the well has been open for an extended period of time which, combined with the heavy mud weight, may have damaged the reservoir rock.

Based primarily upon the results of the Mara C-13 well and in part from this and other wells, Sinclair et al. (1992) defined a group of potential plays. Sinclair et al. (1992) defined them as being the “shale bounded sandstone” group of plays (Figure 2.3). This type of trap possibly occurs anywhere within the Jeanne d’Arc Basin (Sinclair et al., 1992). Although Sinclair does point out the most likely occurrence of gas sands, the large potential area, combined with potentially localized nature of the sand units require more control to be useful.

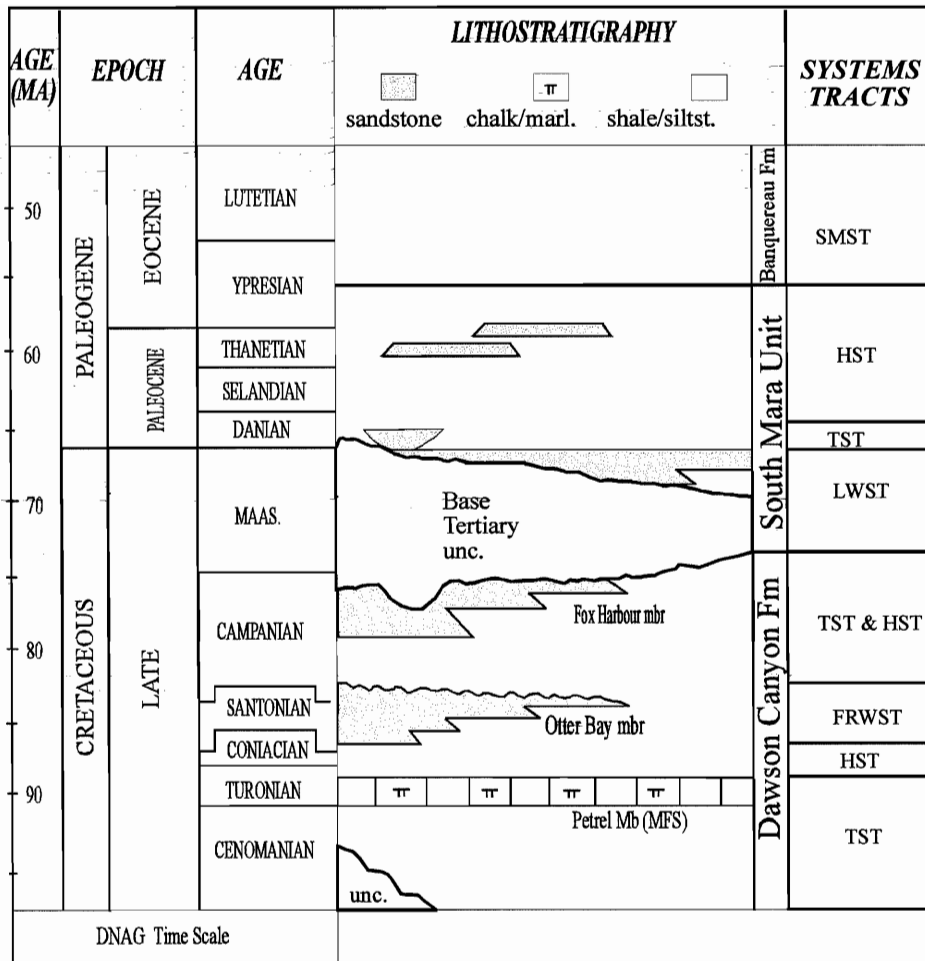


Figure 2.1 Sequence stratigraphic interpretation of the Dawson Canyon Formation and the South Mara Unit from Friis (1997). Note that the predominant location of sand in the South Mara is at the base. Sand stringers located at higher stratigraphic intervals are inferred. See Appendix A for Sequence Stratigraphy definitions. Modified after Friis (1997).

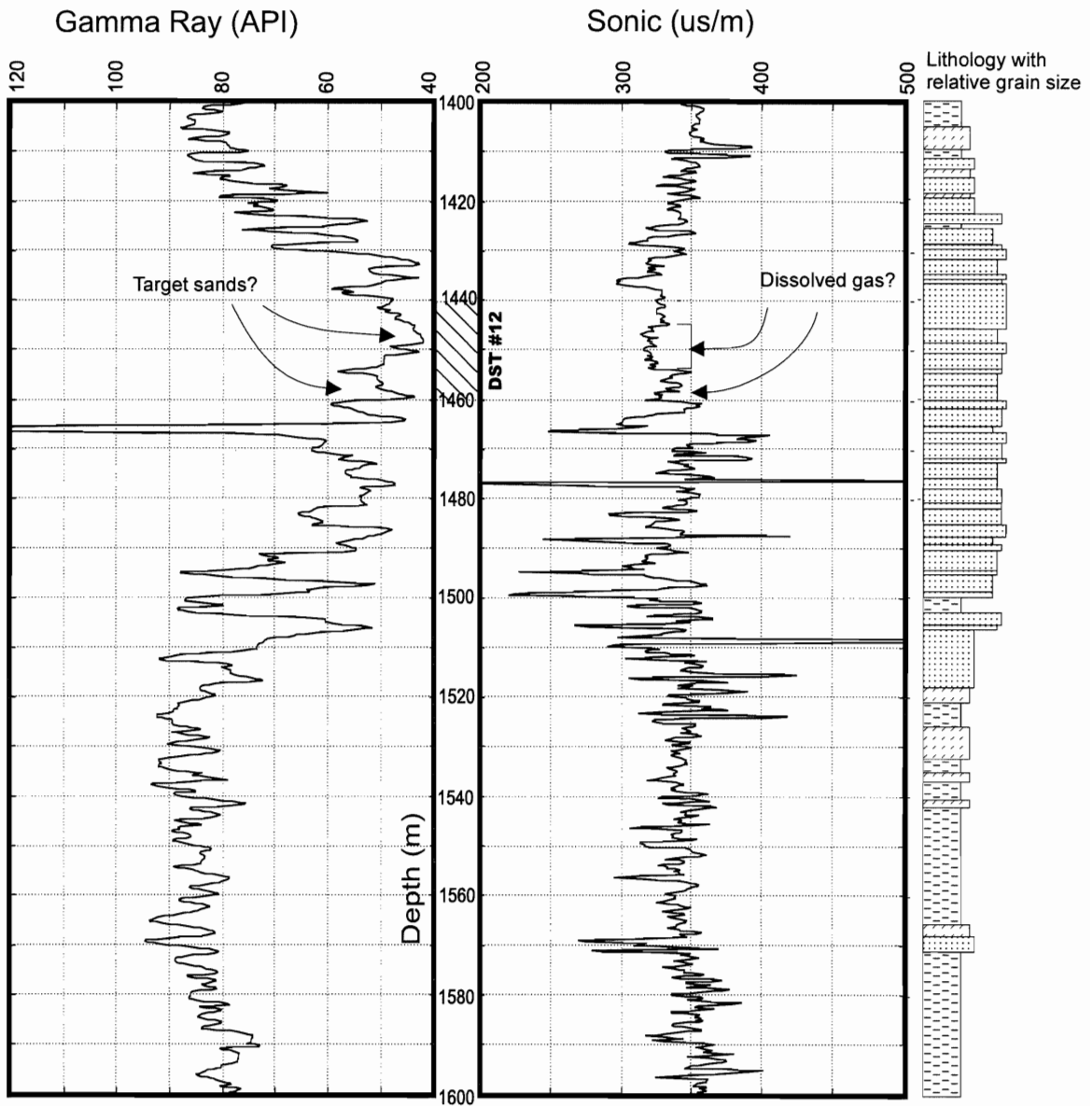


Figure 2.2 Hatched pattern indicates zone that DST #12 was run on. The test produced only water and mud. Testing interval targeted what appears to be 2 sand units with developed porosity. Gas logs indicate maximum dissolved gas levels in excess of 50 ppm, and possibly up to 1-2% dissolved gas. The highly variable sonic log from 1465-1510 m are highly suspect and may indicate a well cave in. (Chevron et al. Hibernia P-15 Well history report, 1979).




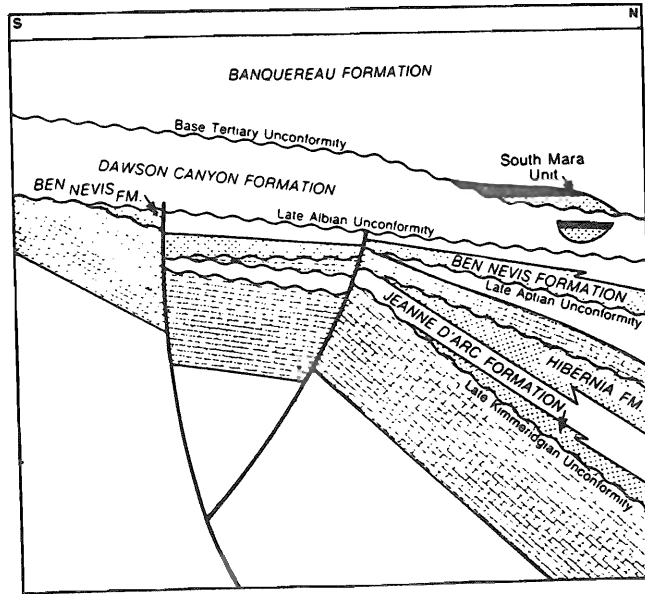
-  Shale
-  Siltstone
-  Sandstone

Figure 2.3 Sinclair et al. (1992) schematic diagram showing the shale bounded sandstone stratigraphic group of plays.



2.3 Geophysical Data

The Hibernia Management Development Corporation¹ provided a 3-D time migrated, decimated version of the original seismic data set, acquired in 1991, to the Geological Survey of Canada-(Atlantic). The decimated version was stored in an 8-bit format with minimal clipping applied to preserve amplitude information. The spacing of the seismic traces is every 25m along the NE-SW and NW-SE directions; i.e. the bin size (see section 3.3) of the data is 25m x 25m. Data coverage near the edge of the survey was poor due to edge effects (low coverage). Figure 2.5 shows the areal coverage of the seismic survey is about 512 km² (Shimeld, pers. comm.).

Seismic data fold (see section 3.3) of the data is not known, but is generally quite good. Also, the actual, detailed processing parameters are not available. The seismic data was sampled at 2 ms.

A limited amount of well wireline log lithological and data is also used in this study. The well data is from the BASIN database, maintained by the GSC-A, and created from the original well reports filed with the CNOPB. Interpretation of the well data from Friis (1997) is used.

¹ A partnership of Mobil Oil Canada (33.125%), Chevron Canada Resources (26.875%), Petro-Canada (20%), Canada Hibernia Holding Corporation (8.5%), Murphy Oil (6.5%), and Norsk Hydro (5%).

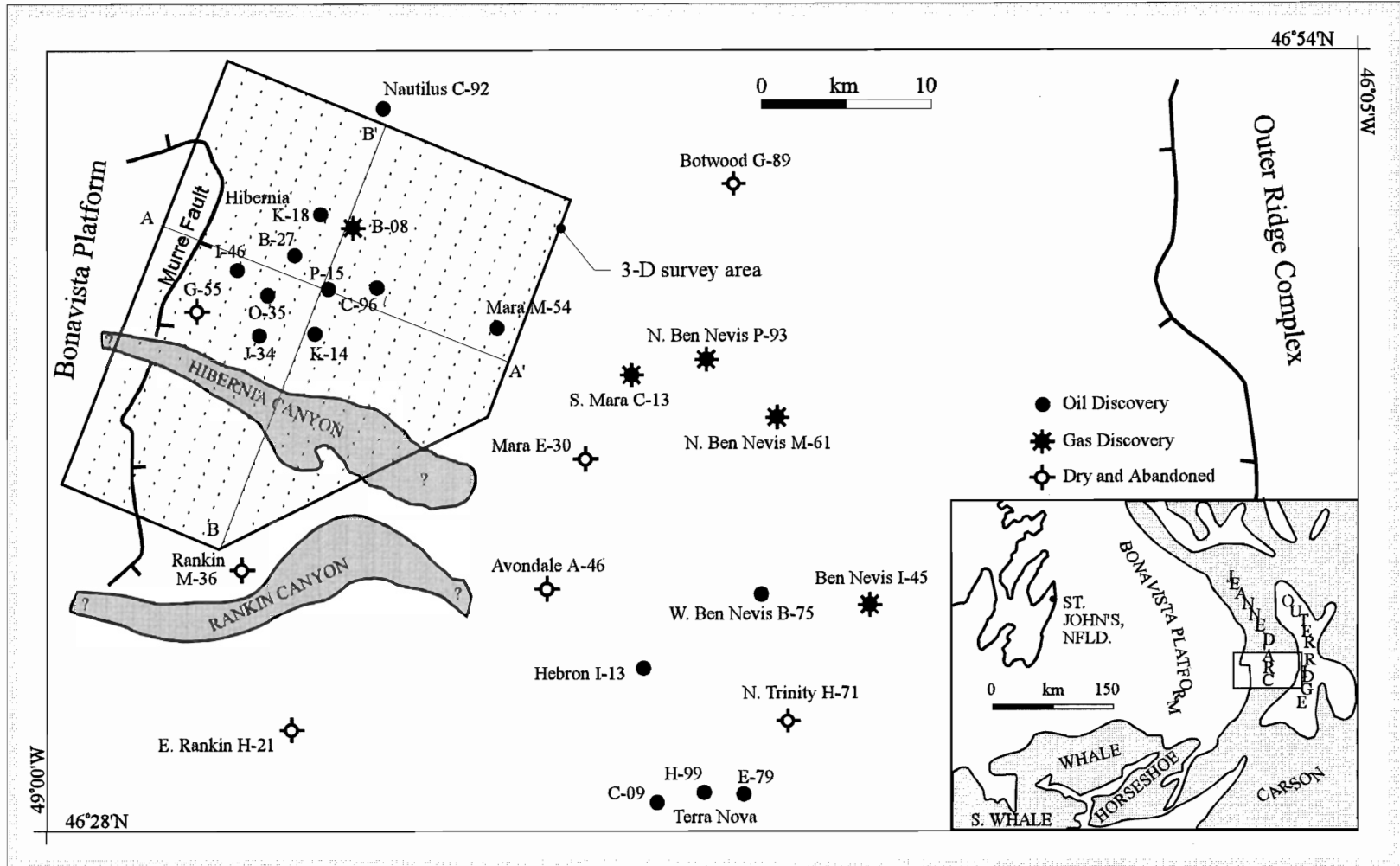


Figure 2.5 Map illustrating location of 3D survey area, Hibernia wells. A-A' and B-B' refer to seismic profiles in Figures 1.1 and 1.2 respectively. Hierbnia Canyon and Rankin canyon are interpreted by K. Dickie. Areal extent of 3D survey is about 512 sq. km (Shimeld, pers. comm). After Friis (1997).

3 THEORETICAL BACKGROUND

This chapter outlines basic theory of the reflection seismic method, and the analytical steps in interpreting the data. After basic reflection seismic concepts are developed, important differences between conventional 2D seismic data and the 3D data used here in this study are provided. The seismic data contains some very important information about environmental information encoded in the reflection geometry and seismic amplitudes. Background to interpret paleo-environment from seismic is presented.

3.1 Reflection Seismology

Seismic reflections profiles are constructed by recording reflections of acoustic energy; these reflections are analogous to sound ‘echoes’. The standard energy source for marine seismic work is the air gun. Arranged in large arrays, they provide a very strong and consistent pulse of energy. This pulse propagates through earth media spherically. Since the earth is anisotropic, the travel path the pulse takes is differentially restricted. This restriction occasionally results in reflections (Telford et al., 1990).

The two most important parameters that determine where the reflections occur are the angle of incidence and acoustic impedance contrast between strata (see Eqn. 3-1). Snell’s Law shows how energy is reflected and transmitted at

stratal interfaces. affecting the apparent subsurface geometry. Zoeppritz's equations describe how energy is partitioned. For wave phenomena, Snell's Law is actually a specific case of Zoeppritz's equations, which more completely describe the partitioning of energy (i.e. reflections) at interfaces (Telford et al., 1990). Telford et al (1990) provides the derivations of Zoeppritz's equations for those interested.

Seismic reflections generally occur at bedding planes or at unconformities, thus representing chronostratigraphic surfaces and not lithostratigraphic surfaces (Boggs, 1987). This results from the fact that lateral changes in lithology are generally gradational, in contrast to sharp changes at bedding planes or unconformity surfaces. Lateral lithologic changes result in a change of reflection characteristics such as amplitude and width (Meckel and Nath, 1977).

How acoustic energy is partitioned at interfaces is also described by Zoeppritz's equations. Those equations involve a great number of variables and are not easy to generalize except for the special case of normal incidence (Figure 3.1). In the case of normal incidence, shear waves B_1 and B_2 are not generated.

Fortunately, this simplification also holds for near-normal incidence as well, allowing it to have great applicability to reflection seismology (Telford et al., 1990; Meckel and Nath, 1977).

The normal incidence form of Zoeppritz's equations determines the relative amplitude of the signal *reflected and transmitted* at an interface. This is a function of the acoustic impedance, Z . Acoustic impedance itself is a product of

the sonic compressional velocity and the bulk density of the medium (Equation 3-1).

$$Z = \rho v \quad (\text{Eqn. 3-1})$$

Where Z is the acoustic impedance [$M / L^2 T^2$] (Telford et al., 1990);

ρ is the bulk density [M / L^3];

v is the sonic compressional velocity [L / T^2].

The relative amplitudes of the normal incident reflection is determined by the contrast in acoustic impedance (Equation 3-2):

$$R = \frac{Z_2 - Z_1}{Z_2 + Z_1} = \frac{\rho_2 v_2 - \rho_1 v_1}{\rho_2 v_2 + \rho_1 v_1} \quad (\text{Eqn. 3-2})$$

Where R is the reflection coefficient [dimensionless] (Telford et al., 1990);

It follows from Eqn. 3-2 that reflections only occur where there is a change in acoustic impedance and not necessarily a change in lithology. Gradational lithologic changes result in gradational acoustic impedance changes. For this reason, they do not produce reflections. Also, the reflection coefficient R is the relative amplitude of the *reflected* seismic pulse; the amplitude of the transmitted pulse is in Eqn. 3-3.

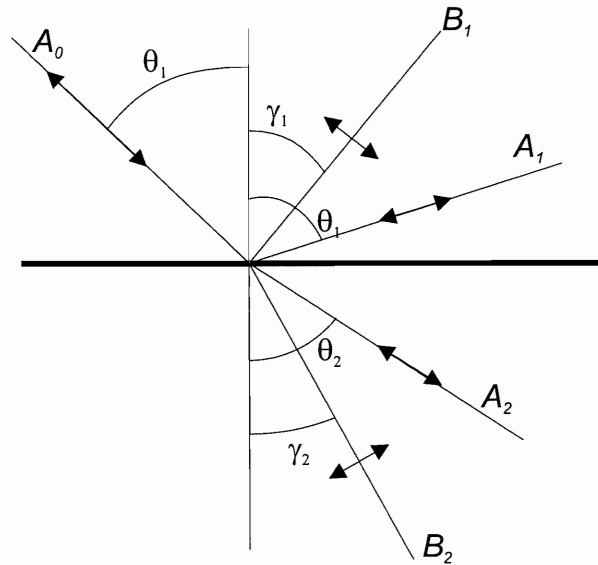
$$T^2 = 1 - R^2 \quad (\text{Eqn. 3-3})$$

Where T is the relative amplitude of the transmitted pulse [dimensionless] (Telford et al., 1990);

The energy of the reflected and transmitted signals is proportional to the amplitude squared (Telford et al., 1990). An important implication of the energy partitioning, combined with all the other energy loss mechanisms (See Table 3.1), is that reflections at depth are progressively represented by weaker and weaker reflections, even though reflections from deeper interfaces may have higher reflection coefficients than shallower reflections. Correctly compensating for the loss of energy due to the effects outlined in Table 3.1, and thus preserving the relative reflection amplitudes, is exceedingly important to properly estimate the seismic character (see section 3.3). At present amplitude processing usually only includes corrections for spherical divergence, with an additional scalar to compensate for acquisition parameters (Yilmaz, 1987).

Figure 3.1 Partitioning of amplitude at an interface.

Waves generated at an interface by an incident P wave.



- A_0 - Incident P Wave
- A_1 - Reflected P Wave
- A_2 - Transmitted P Wave
- B_1 - Reflected S Wave
- B_2 - Transmitted S Wave
- θ_1 - Incident and reflected P wave angle
- θ_2 - Refracted P wave angle
- γ_1 - Reflected S wave angle
- γ_2 - Transmitted S wave angle

Table 3.1 Mechanisms for energy loss

Spherical Divergence as sound energy travels in all directions at once.
Preferential absorption of higher frequencies by inelastic deformation of rocks.
Reflection of energy to the surface, preventing less energy to travel to depth.
Scatter of energy by inhomogeneities.

3.2 2D vs 3D Seismic Data

This project uses 3D seismic data which, in a very limited sense, is similar to a very dense collection of 2D seismic lines. Instead of hundreds of meters or even kilometers between lines, line spacing is reduced to 25m or even less. The line density itself allows for much more control in interpretation. Advanced processing and display techniques has allowed much more detailed information to be extracted from the seismic data than merely viewing it as a collection of tightly spaced 2D seismic lines. In particular, processing all of the data as one 3D *volume* of data instead of discrete 2D *planes* offers considerable improvements in lateral resolution. Migration is one of the principal processing techniques for improving lateral resolution (Kearney and Brooks, 1984; Yilmaz, 1987). Migration, as its name implies, repositions reflections to their true subsurface locations and focuses energy in the Fresnel zone to a much smaller area (Figure 3.2). The Fresnel zone is the horizontal area that reflects back energy towards the surface (Kearney and Brooks, 1984). Out of plane reflected energy is minimized more than in the 2D case. Less interference results in a more reliable interpretation, and smaller features can be confidently identified.

Both the acquisition (e.g. line spacing) and subsequent processing, in particular 3D migration, affect the lower limit on the size of a recognizable feature. In general, resolution increases with tighter line spacing and a greater frequency content in the data (Yilmaz, 1987; Robertson and Nogami, 1984). For

area resolution, both of these factors affect the Fresnel zone (Figure 3.2). Under ideal conditions and processing, the horizontal resolution of a 3D survey approaches that of the horizontal bin spacing (Brown, 1996). For the 3D survey in this study, the bin spacing is about 25 m, so the minimum size of an object to generate a distinct reflection is:

$$\text{minimum size} = \pi r^2 = \pi \cdot (25 \text{ m})^2 \cong 2000 \text{ m}^2 \quad (\text{Eqn. 3-4})$$

Objects below this limit reflect energy but do not produce a distinct reflection but they may modify the amplitude of nearby reflections.

Kallweit and Wood (1982) and others have done extensive work on the lower limit of vertical resolution of seismic signals. Both Kallweit and Wood (1982) and Robertson and Nogami (1984) have demonstrated that reflectors at a spacing below a threshold, will interfere with each other. The distance separating the two reflectors is encoded within the amplitude of the reflection. This phenomena, called tuning, is discussed in section 3.4.2.

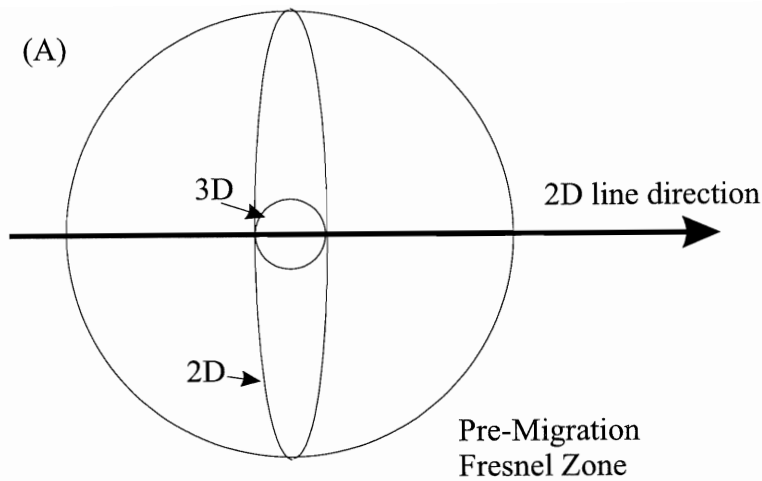


Figure 3.2 Pre-Migration Fresnel zone compared with 2D and 3D migration. The assymetrical shape of the 2D migration Fresnel zone contributes much out-of-plane energy. Modified from Brown, A.R. (1996).

The areal coverage of a 3D survey compared with a grid of five 2D lines. The combination of dense sampling and better Fresnel zone control improves resolution considerably. The meanders here would not be resolvable with just 2D seismic coverage (larger black dots).

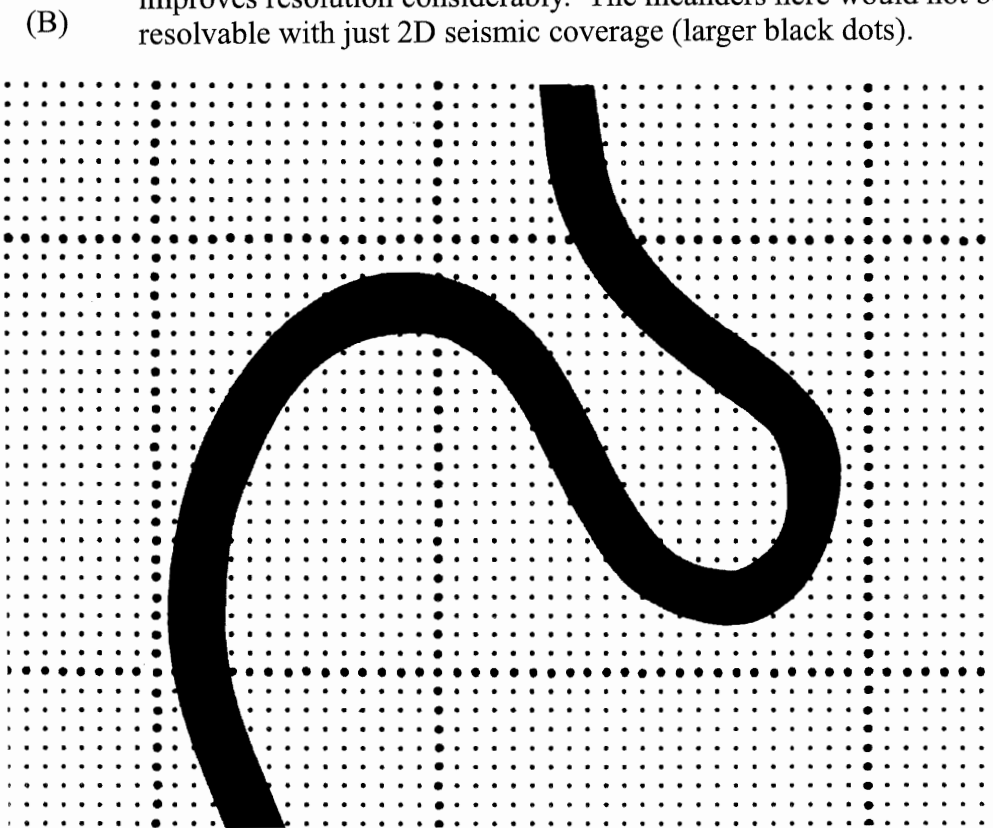
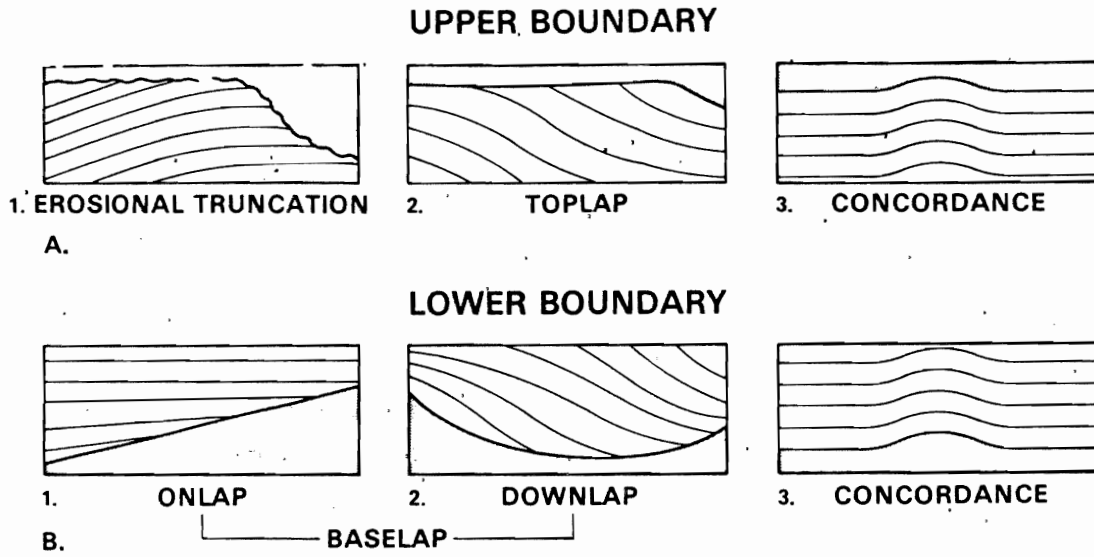


Figure 3.3 Stratal geometric relationships at sequence boundaries



3.3 Seismic Stratigraphy

With the improvement of reflection seismic acquisition and processing technology in the 1970s, Peter Vail and others were able to apply concepts from Sloss (1963) to interpret stratigraphy from seismic data. Sequence stratigraphy, developed by Sloss, attempts to subdivide, interpret and correlate sedimentary rocks into units called sequences. A sequence is a relatively conformable, genetically related succession of strata bounded by chronostratigraphically significant surfaces, called sequence boundaries (Boggs, 1987). Sequence boundaries are unconformities and their correlative conformities. Sequence boundaries can usually be distinguished by characteristic geometry.

Figure 3.3 shows schematic stratal relationships at lower and upper surfaces of sedimentary sequences. Seismic methods are more adapted to reveal geometric relationships. Therefore, it is difficult, if not impossible, to discern concordant sequence boundaries by seismic data alone, unless the concordant surfaces are correlated to a reflection exhibiting any of the other four angular relationships.

Combining the geometric information with amplitude information makes it possible to arrive at some limited environmental interpretation. This is summarized in Table 3.2

Table 3.1 Seismic characteristics and Environmental Facies Interpretation of Clastic Facies Units (From Sangree and Widmier, 1977).

DEPOSITIONAL FRAMEWORK INTERPRETATION	SEISMIC FACIES UNIT	ENVIRONMENTAL FACIES INTERPRETATION	EXTERNAL FORM OF FACIES UNIT	REFLECTION GEOMETRY AT BOUNDARIES	REFLECTION CONFIGURATION		LATERAL RELATIONS	OTHER SEISMIC FACIES PARAMETERS			
					PRINCIPAL INTERNAL CONFIGURATION	CONFIGURATION MODIFIER		INTERVAL VELOCITY	AMPLITUDE	CONTINUITY	FREQUENCY (CYCLE BREADTH)
SHELF	HIGH-CONTINUITY AND HIGH-AMPLITUDE	TYPICALLY SHALLOW MARINE CLASTICS DEPOSITED PRIMARILY BY WAVE TRANSPORT PROCESSES. COULD ALSO BE FLUVIAL CLASTICS INTERBEDDED WITH WIDESPREAD MARSH DEPOSITS	SHEET OR WEDGE	CONCORDANT AT TOP WITH CONCORDANT TO GENTLE ONLAP OR DOWNLAP AT THE BASE	PARALLEL TO DIVERGENT		MAY GRADE Laterally TO ALL OTHER SHELF FACIES OR TO UNDAFORM PORTION OF SLOPE PROGRADATIONAL FACIES		RELATIVELY HIGH BUT VARIABLE	RELATIVELY CONTINUOUS	VARIABLE, SOME BROAD CYCLES
SHELF	LOW-AMPLITUDE	MARINE CLASTICS DEPOSITED BY LOW-ENERGY TURBIDITY CURRENTS AND BY WAVE TRANSPORT	SHEET OR WEDGE	CONCORDANT AT TOP WITH CONCORDANT TO GENTLE ONLAP OR DOWNLAP AT THE BASE	PARALLEL TO DIVERGENT		MAY GRADE Laterally TO SLOPE PRO GRADATIONAL FACIES OR TO HIGH CONTINUITY AND HIGH AMPLITUDE SHELF FACIES		VERY LOW TO LOW	DISCONTINUOUS TO CONTINUOUS	VARIABLE BUT LACKS EXTREMES OF HIGH-CONTINUITY AND HIGH-AMPLITUDE FACIES
		FLUVIAL AND NEARSHORE CLASTICS DEPOSITED BY FLUVIAL AND WAVE TRANSPORT PROCESSES					MAY GRADE Laterally TO HIGH CONTINUITY AND HIGH-AMPLITUDE OR TO LOW CONTINUITY AND VARIABLE AMPLITUDE SHELF FACIES		LOW	DISCONTINUOUS TO MODERATELY CONTINUOUS	
SHELF	LOW-CONTINUITY AND VARIABLE AMPLITUDE	DOMINANTLY NON-MARINE CLASTICS. DEPOSITED BY RIVER CURRENTS AND ASSOCIATED MARGINAL MARINE TRANSPORT PROCESSES	SHEET OR WEDGE	CONCORDANT AT TOP WITH CONCORDANT TO GENTLE ONLAP OR DOWNLAP AT THE BASE	PARALLEL TO DIVERGENT		COMMONLY GRADES Laterally TO HIGH CONTINUITY AND HIGH AMPLITUDE FACIES OR TO SAND PRONE LOW AMPLITUDE FACIES		LOW TO HIGH, QUITE VARIABLE WITH FREQUENT BURSTS OF HIGH AMPLITUDE	GENERALLY DISCONTINUOUS TO MODERATELY CONTINUOUS	QUITE VARIABLE
SHELF	MOUNDED	SHELF DELTA COMPLEX	LOW MOUND OR ELONGATE MOUND	CONCORDANT AT TOP WITH GENTLE DOWNLAP AT BASE	MOUNDED TO SIGMOID AND DIVERGENT		COMMONLY GRADES Laterally TO HIGH CONTINUITY AND HIGH AMPLITUDE FACIES OR TO UNDAFORM PORTION OF SLOPE PROGRADATIONAL FACIES		VARIABLE BUT RELATIVELY LOW BURSTS OF DISCONTINUOUS HIGH AMPLITUDE ARE COMMON	DISCONTINUOUS TO MODERATELY CONTINUOUS	QUITE VARIABLE, SOME NARROW CYCLES

DEPOSITIONAL FRAMEWORK INTERPRETATION	SEISMIC FACIES UNIT	ENVIRONMENTAL FACIES INTERPRETATION	EXTERNAL FORM OF FACIES UNIT	REFLECTION GEOMETRY AT BOUNDARIES	REFLECTION CONFIGURATION		LATERAL RELATIONS	OTHER SEISMIC FACIES PARAMETERS			
					PRINCIPAL INTERNAL CONFIGURATION	CONFIGURATION MODIFIER		INTERVAL VELOCITY	AMPLITUDE	CONTINUITY	FREQUENCY (CYCLE BREADTH)
SHELF-MARGIN AND PROGRADED-SLOPE	SIGMOID-PROGRADATIONAL	CLAY MUDDS DEPOSITED BY LOW ENERGY TURBIDITY CURRENTS AND BY HEMIPELAGIC DEPOSITION FROM LOW VELOCITY WATER CURRENTS SHELFAL UNDAFORM PORTIONS MAY INVOLVE WAVE AND EVEN FLUVIAL TRANSPORT PROCESSES	ELONGATE LENS TO SUBTLE FAN	CONCORDANT AT THE TOP WITH DOWNLAP AT THE BASE	SIGMOID ALONG DEPOSITIONAL DIP AND PARALLEL TO SUB PARALLEL ALONG DEPOSITIONAL STRIKE		MAY GRADE LATERALLY OR VERTICALLY TO OBLIQUE PROGRADATIONAL FACIES COMMONLY ONLAPPED BY ONLAP FILL FACIES UNDAFORM PART MERGES WITH SHELF FACIES AND FONDIFORM FAULT MAY GRADE TO SHEET DRAPE FACIES	GENERALLY MODERATE TO HIGH, RELATIVELY UNIFORM	NORMALLY CONTINUOUS	VARIES PARALLEL TO DIP WITH BROADEST CYCLES ASSOCIATED WITH THICKER BEDS OF THE MIDDLE CLINOFORMING ZONE CYCLE BREADTH IS UNIFORM ON SECTIONS PARALLEL TO DEPOSITIONAL STRIKE	
SHELF-MARGIN AND PROGRADED-SLOPE	OBLIQUE-PROGRADATIONAL										
	SUBZONES UNDAFORM	SEDIMENT COMPLEX USUALLY DEPOSITED IN SHELF-MARGIN DELTAIC ENVIRONMENT INCLUDES DELTA PLAIN, DELTA FRONT AND PRODELTA PROCESSES MAY ALSO BE FORMED IN DEEP WATER ASSOCIATED WITH STRONG BOTTOM CURRENTS	FAN	CONCORDANT AT TOP IF UNDAFORM CYCLES PRESENT	PARALLEL		COMMONLY MERGES DOWNDIP WITH DEEP BASIN TURBIDITES, MASS TRANSPORT AND HEMIPELAGIC FACIES FREQUENTLY ONLAPPED BY ONLAPPING FILL FACIES MAY GRADE LATERALLY OR VERTICALLY TO SIGMOID-PROGRADATIONAL FACIES UNDAFORM POSITION MERGES WITH PARALLEL LAYERED SHELF FACIES	MODERATE TO HIGH	GENERALLY CONTINUOUS	RELATIVELY UNIFORM	
	UPPER CLINOFORM			TOPLAP TRUNCATION AT THE TOP	OBLIQUE ALONG DEPOSITIONAL DIP AND PARALLEL OR GENTLY OBLIQUE TO SIGMOID PARALLEL TO DEPOSITIONAL STRIKE	MODERATE TO HIGH		GENERALLY MODERATELY CONTINUOUS	FAIRLY UNIFORM		
	MIDDLE AND LOWER CLINOFORM			DOWNLAP AT THE BASE		VARIABLE GENERALLY LOWER THAN OTHER SUBZONES		DISCONTINUOUS TO MODERATELY INCREASES TOWARD LOWER CLINOFORM ZONE	CYCLE BREADTH DECREASES RAPIDLY DOWNDIP AS BEDS THIN		
						GENERALLY MODERATE TO LOW		CONTINUOUS	RELATIVELY NARROW CYCLE BREADTH DECREASES BASINWARD		
FONDIFORM											
BASIN-SLOPE AND BASIN-FLOOR	SHEET DRAPE	DEEP MARINE HEMIPELAGIC CLAYS AND OOZES	SHEET DRAPE	CONCORDANT AT TOP AND CONCORDANT OR VERY SLIGHT ONLAP AT BASE	PARALLEL		COMMONLY INTERBEDDED WITH TURBIDITE SANDS & SILTS, AND GRADES TO GENTLY DIVERGENT FONDIFORM SEDIMENTS OF PROGRADING COMPLEXES	COMMONLY RELATIVELY LOW TO MODERATE	CONTINUOUS	NORMALLY UNIFORM NARROW	
BASIN-SLOPE AND BASIN-FLOOR	SLOPE-FRONT FILL	DEEP-WATER SEDIMENT COMPLEX COMMONLY RELATED TO SUBMARINE FANS	LARGE FAN	CONCORDANT AT TOP ONLAPS UPDIP AND DOWNLAPS DOWNDIP	PARALLEL TO SUBPARALLEL		THINS AND GRADES INTO BASIN FLOOR FACIES, COMMONLY PINCHES OUT UPDIP	VARIABLE	VARIABLE	VARIABLE	
BASIN-SLOPE AND BASIN-FLOOR	ONLAPPING FILL	RELATIVELY LOW VELOCITY TURBIDITY CURRENT DEPOSITS	BASIN TROUGH CHANNEL AND SLOPE FRONT FILL	ONLAP AT THE BASE AND USUALLY CONCORDANT AT THE TOP			COMMONLY GRADES TO MOUNDED ONLAP OR CHAOTIC FILL FACIES ALTERNATION WITH OTHER FILL FACIES IS COMMON	VARIABLE	COMMONLY CONTINUOUS	CYCLE BREADTH INCREASES INTO FILL CENTER TRENDS TO BE RELATIVELY NARROW	

3.4 Direct Hydrocarbon Indicators

Direct hydrocarbon indicators (DHI) refer to four distinct seismic features that normally indicate the presence of gas and gas/liquid. They have far greater applicability for gas detection than for oil detection because acoustic impedance contrast for gas is generally much greater than for oil.

The DHIs are:

- *Bright spots* are a result of reflections from abnormally high impedance contrasts between gas-saturated sands and the surrounding rocks. In seismic section, they often appear as very strong reflections.
- *Dim spots* occur where water-saturated sands would normally have higher acoustic impedance than the surrounding shales and thus are imaged directly. The introduction of gas into the sand lowers the acoustic impedance and the reflection dims, producing the dim spot.
- *Phase changes* occur when the introduction of gas changes the acoustic impedance of the sand from higher than the surrounding shales to a value lower than the surrounding shales. Since the acoustic impedance contrast from the gas and water saturated sands are of opposite polarity, a phase change develops.
- *Flat spots* normally occur where sand units become sufficiently thick so that a gas/liquid contact develops.

Without preservation of relative amplitudes during processing, it would not be possible for bright or dim spots to be identified. The relative acoustic impedances that produce each of these DHIs are shown in Figure 3.4.

Telford et al. (1990) stated that small amounts of gas can produce a more prominent bright spot than large amounts, or zero amount, of gas accumulation. It is difficult to see how this may be the case. However, it is speculated that Telford et al. (1990) may be referring to shallower, and typically smaller, accumulations of gas, in comparison to the deeper gas accumulations, which harbour the larger accumulations.

In addition, the bright spot DHI is usually only effective for young (Tertiary) sediments only. Older sediments are more compacted and harder and porosity is often lower, reducing the acoustic impedance contrast necessary for bright spots.

Figure 3.4 Schematic Diagram of reservoirs for different acoustic impedance contrasts between the reservoir and the embedding medium. All DHI's show flat spots if a gas/fluid contact exists. Modified from Brown, 1996.

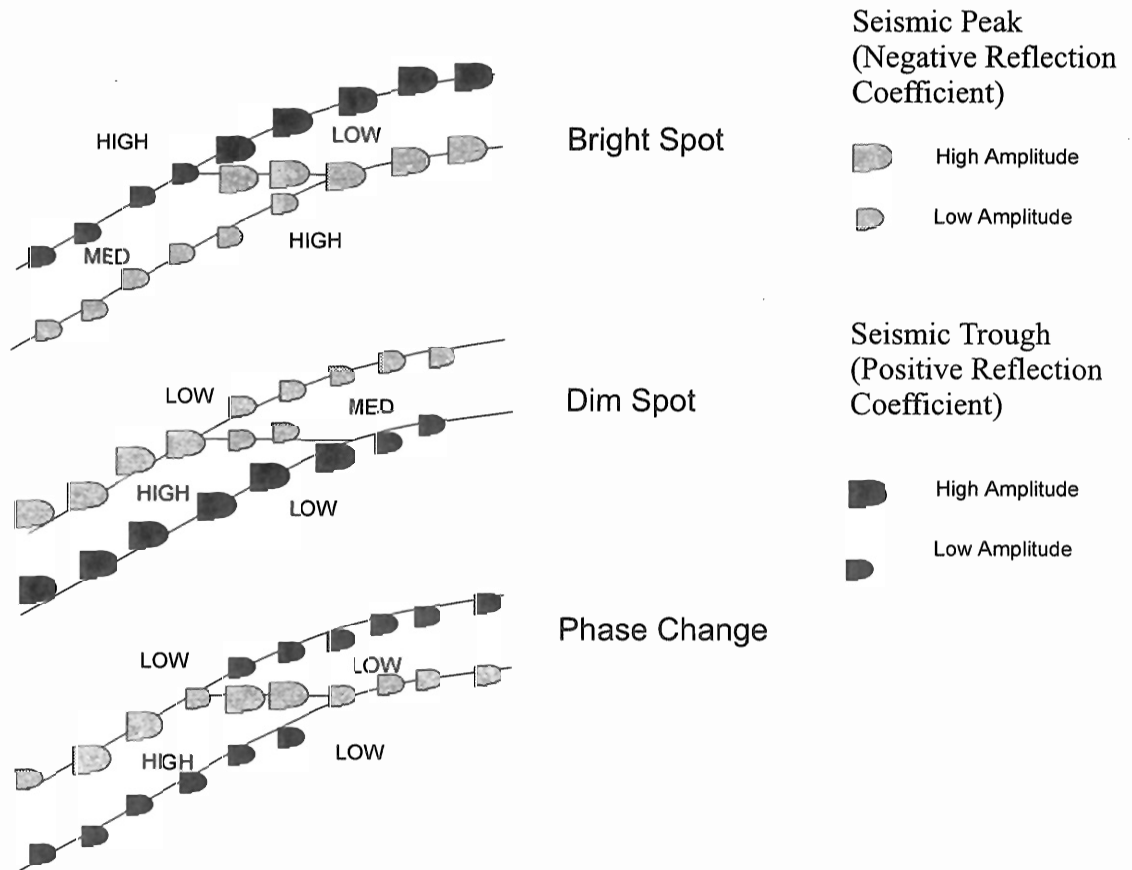


Figure 3.5 Seismic model of tuning occurring at a sand wedge. This diagram shows the relationship between dominant seismic wavelength and bed thickness. A basic 25 Hz Ricker wavelet is used in the model. From Robertson and Nogami (1984).

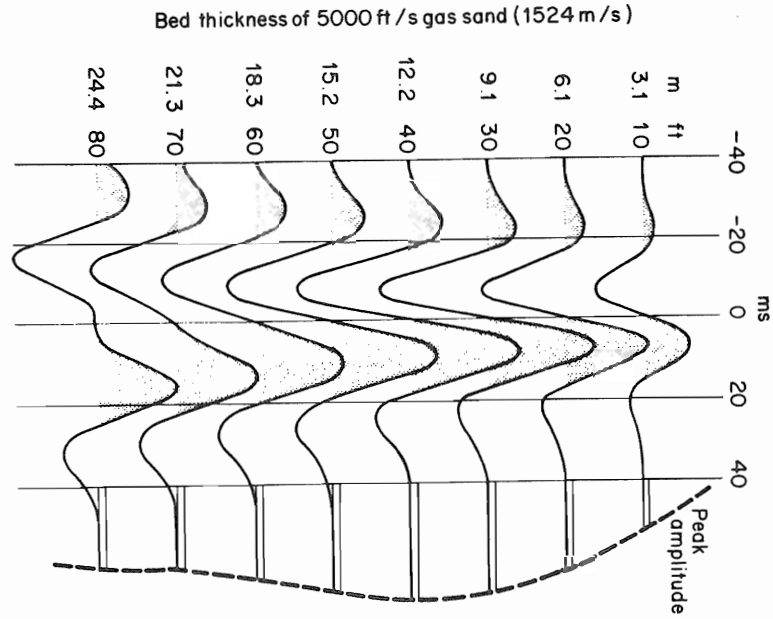


Figure 3.6 Tuning curves for two zero phase wavelets. There is a dependence on the wavelet used, but below the 'tuning thickness', the amplitude changes considerably while apparent thickness does not change appreciably. From Robertson and Nogami (1984).

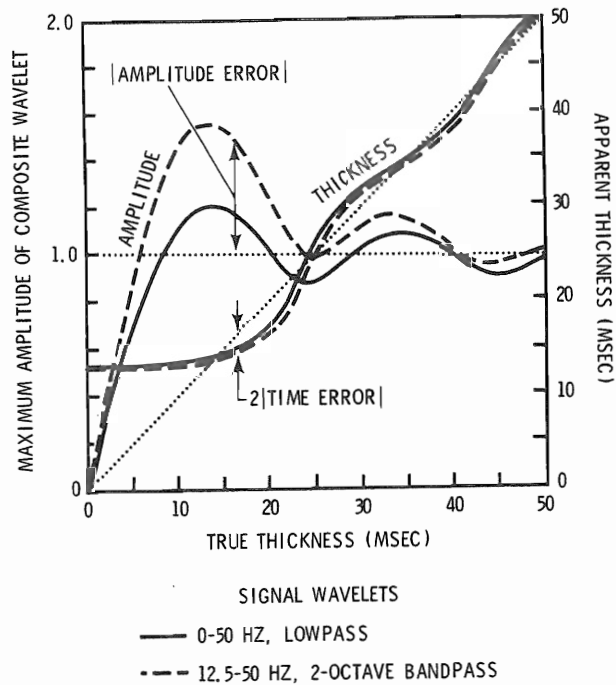


Figure 3.7 Some possible structural traps. From Hamblin (1990).

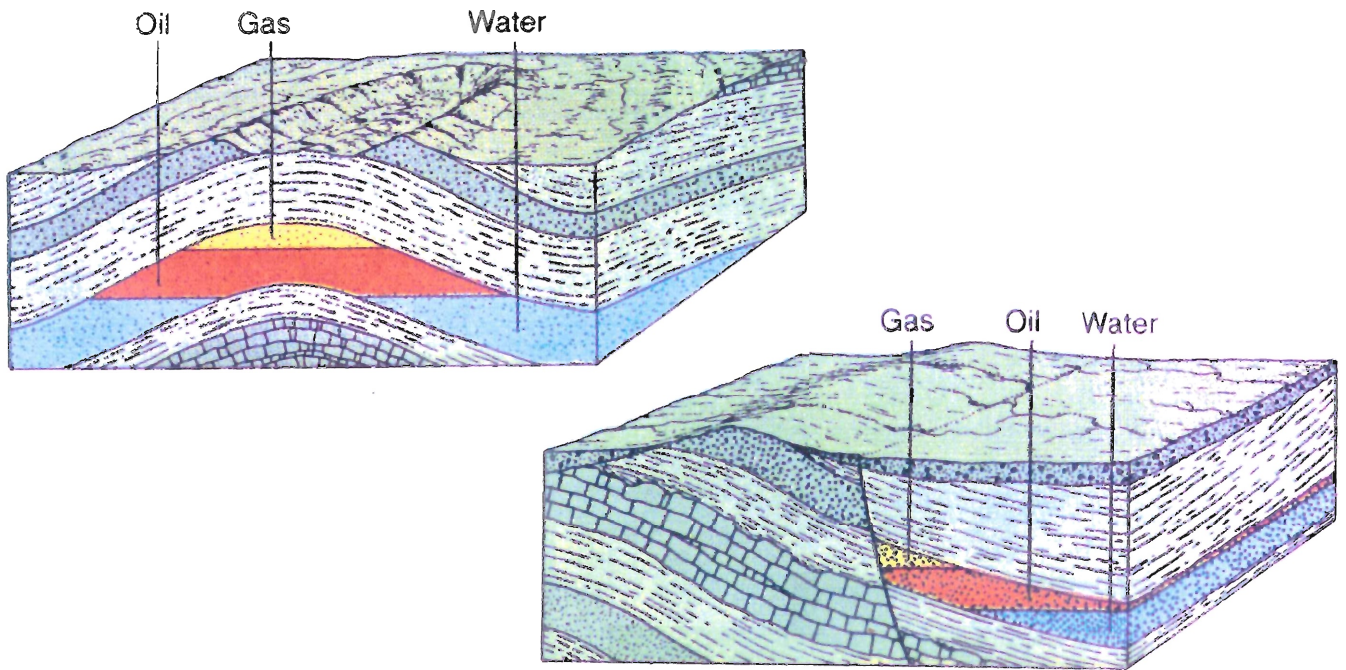
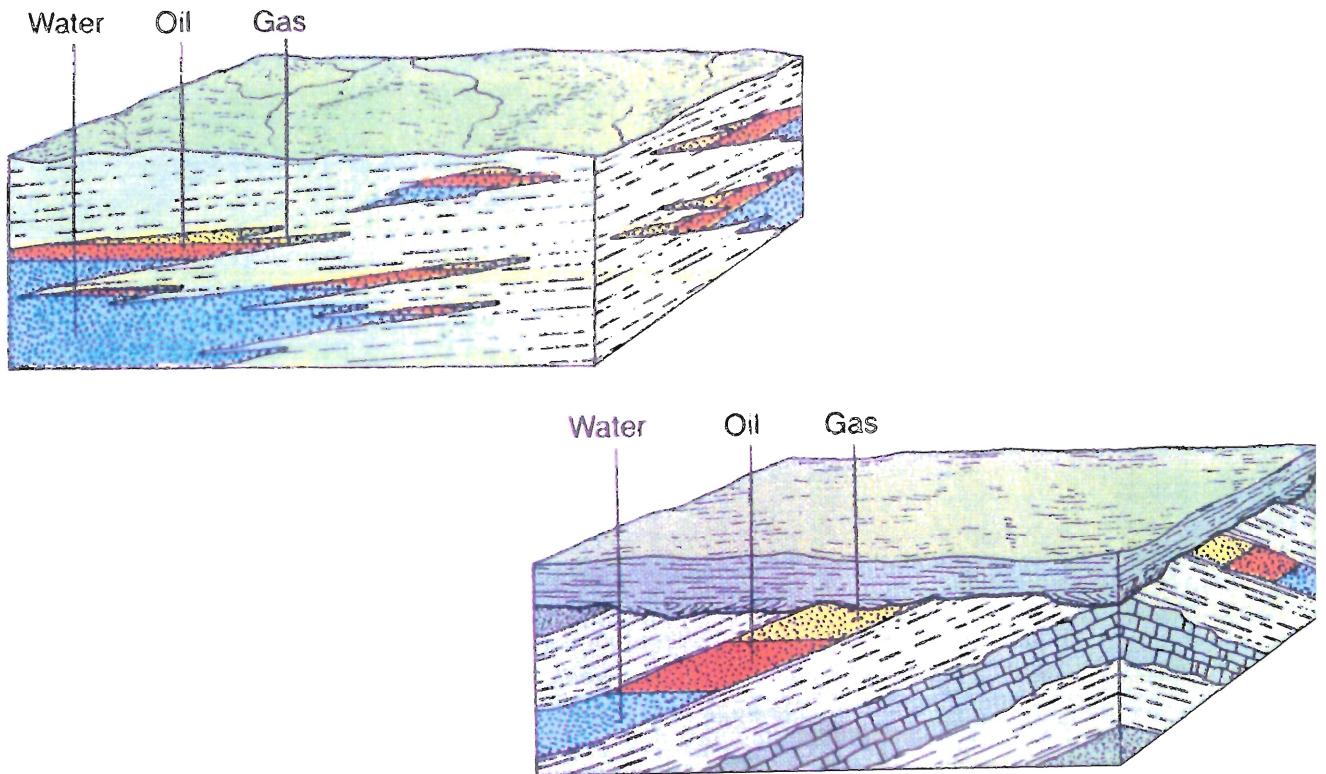


Figure 3.8 Some sample stratigraphic traps. From Hamlin (1990).



3.4.1 Other Causes of Amplitude Anomalies

Some lithologies often produce high amplitude reflections because of anomalously high acoustic impedance contrasts. In particular, coal often produces high amplitude reflections. Typical densities around 1.5-2 g/cm³ and high sonic travel time (400-600 μ s) produces a high contrast with most other lithologies (Schlumberger, 1987). In some areas, such as the Gething and Falher formations in the Western Canadian Sedimentary Basin, often have very localized coal beds. Even thin coal beds may result in strong, high amplitude reflections. These can only be identified by detailed knowledge of the local geology. Lithologies such as coal are not known to occur in significant quantities at Hibernia.

3.4.2 Tuning Effects

Robertson and Nogami (1984) have demonstrated that reflectors within a certain distance of each other will not yield distinct reflections. Instead, the reflection from each of the reflectors will interfere with each other and produce a composite reflection. This phenomenon is known as tuning, and it is highly dependent upon the spacing of the reflectors, the physical properties of the rock, as well as the seismic wavelet. If the waveform is different, then the seismic expression will be different.

Modeling of the tuning effect between beds of different thicknesses shows that there is a systematic change in amplitude of the reflection (Figure 3.2).

Figure 3.3 summarizes the observed effects from tuning, and it is evident that if two units were at a specific distance apart, may result in a stronger seismic response because of tuning than either of the individual reflections.

3.5 Well Information

Two types of well data are used in this study: lithologic information and geophysical well log measurements. Lithologic data is obtained from well cuttings ('chip samples') and from interpretation of geophysical well logs. There is a progressively increasing delay between the time the rock chips are cut and the time they are gathered up at the surface. Therefore, it is possible for the chip samples to become mixed or contaminated, decreasing resolution and accuracy. Despite this, they are useful and provide direct information about subsurface rocks.

Geophysical well logs provide more control, but they only represent some physical properties of the rocks. The two logs used in this study are the gamma ray log and the sonic log.

3.5.1 Gamma Ray Log

The gamma ray log records the natural emission of gamma rays from uranium, thorium, and potassium. The principle radioactive isotope is ^{40}K . The unit of measurement is the API unit, named about the American Petroleum Institute, and defined in a reference well in Houston (Schlumberger, 1987). Clays

often have a much higher capacity to absorb the heavy minerals which have radioactive isotopes than most other sediments, and this leads to the gamma ray log being used as a “shale indicator”. Quartz, often the last mineral to break down, is the predominant mineral in many sandstones and shows almost no natural radioactivity. So in general, the greater the background radiation, the more ‘shale’ is inferred to be present.

However, most sands have varying amounts of radioactive minerals such as feldspars and micas, and may indicate high ‘shale’ content even if there is abundant coarse grained sediments present. Also, some clays such as kaolinite and montmorillonite are less radioactive than many other clay minerals and may result in misinterpretations so other logs and well cuttings should be used to constrain possible lithology. Also, carbonates are not very naturally radioactive, and a carbonateaceous mud may look like ‘sand’, emphasizing the need to use other logs for lithologic interpretation.

The fact that rocks can have widely varying lithologies means that for practical interpretation of what is ‘sandy’ and what is ‘shaley’ in clastic sequences, some well cuttings would have to be known. For example if a quartzite (or otherwise ‘clean sand’ is available within close proximity to the sequence under consideration, then that could be used to estimate how ‘clean’ other sands are within the same sedimentary sequence. This would not be possible without using well cuttings as reference, or without knowing that a particular unit is “clean”.

3.5.2 Sonic Log

The sonic log measures the acoustic interval velocity. This log actually measures the time it takes for sound to travel along a certain distance in the sidewall rock, and thus has units of $\mu\text{s/m}$ (dimensions of $[T/L]$). Inverting this number gives the interval velocity. Different lithologies have a characteristic range of velocities, but applying sonic logs to differentiate lithology is generally not possible because shale and sand often have very similar velocities when buried to any depth. However, carbonate sequences can usually be identified quite readily since carbonates often have much higher velocities than clastic sediments.

Sound waves travel better through more dense material. This makes sonic logs also useful as indicators of formation porosity. Once lithology is constrained within an interval, porosity can be observed as a decrease in velocity (or an increase in interval time).

3.6 Trap Types

All economic occurrences of hydrocarbons require a mechanism in which the hydrocarbons can accumulate. There are two broad groups of traps where hydrocarbons can accumulate:

- *Structural Traps* result from deformation of the earth so that reservoir rocks have some form of *structural closure* by surrounding sealing rocks. Closure is the case where, above a vertical level, the reservoir rocks are completely surrounded by sealing rocks. The amount of closure is the difference in this level to the top of the reservoir rock (Figure 3.7). This broad group can be further subdivided into the mechanisms of deformation, namely:
 1. *Fold related structural traps* – these result when vertical closure is created by antiformal deformation, and they can occur in either compressional or extensional regimes.
 2. *Fault related structural traps* – these occur when permeable, reservoir quality rocks are juxtaposed against sealing rocks. However, faulting may not necessarily result in a seal. There is a requirement that there be enough sealing ‘grout’ in the fault gouge so that the fault plane does not represent a potential migration route.
- *Stratigraphic Traps* are often known as ‘subtle’ traps because they are not as evident as structural traps since they result from lithostratigraphic changes. Seismic reflections, on the other hand, usually represent chronostratigraphic surfaces. (Figure 3.8)

3.7 Software and Hardware

The primary suite of software used in this project is Landmark Graphics Corporation's EarthCube v1.2 suite, which includes SeisWorks/3D and SeisCube. The EarthCube suite is Unix based and runs mainly on Sun's Solaris or SGI's IRIX platforms. Interpretation was primarily accomplished using SeisWorks/3D on a Sun SparcStation 20, while SeisCube made extensive use of the graphical hardware of an SGI Indigo2 with a MIPS R4400 processor and Maximum Impact Graphic hardware.

Seisworks/3D is the primary interpretation package and is typical of industry standard, conventional interpretation software. Data can be displayed in inline or crossline directions or in any arbitrary direction. Horizontal and horizon-parallel time slices are also permitted with interactive interpretation available in any view.

SeisCube displays data as a volume and not as discrete planes extracted from the data cube. Interpretation is possible not only along any plane, but also in distinct paths. It makes it easier to visualize the 3D geometry during interpretation. However there is considerable hardware overhead required to use these features so SeisCube is mainly used to check and display interpretations from SeisWorks/3D. A particular strong advantage of SeisCube is its ability to view *all* of the data simultaneously. In particular, tools such as the opacity mapping tool means that you can directly observe 3D relationships of interpreted

features in conjunction with the seismic data. Adjusting perspective and transparency values can vary how 'far' you see into the cube.

4 SEISMIC INTERPRETATION

Interpretation of the seismic was conducted based upon the principles presented in Chapter 3. The following sections present the interpretation based almost exclusively on the seismic data; Chapter 5 uses some additional well data to augment the seismic data.

4.1 Work Flow

The two horizons were manually picked using a 1km x 1km grid of in- and cross- lines through the 3D survey. The seismic was then autopicked throughout the 3D dataset using ZAP III. This interpretation was examined, and the original picks were then manually edited and repicked on a ½ km x ½ km grid and then autopicked again through the dataset. Subsequent repicking/autotracking cycles used ¼ km x ¼ km and 100m x 100m grids. This last autopicked horizon was then subsequently edited by hand and smoothed with a 5 x 5 trace matrix.

4.2 Mapped Horizons

The South Mara Unit is bounded above and below by unconformities (Figure 4.1 and Figure 4.2). The base of the South Mara Unit is the regional Base Tertiary Unconformity (BTU). The top of the South Mara is interpreted here to be an unconformity surface. There is no formal nomenclature for this

unconformity, although it has been recognized by a number of authors, including McAlpine (1990b), so it has tentatively been named Unconformity A (UA).

Figure 4.3 shows the map view and a plan view of the BTU. The BTU overlies the deltaic successions of the Dawson Canyon Formation. Within the 3D survey, only the Otter Bay Member of the Dawson Canyon Formation is present; the Fox Harbour Member is not very well developed here. Considerable erosion is associated with the BTU. The reflection amplitude of the BTU is generally quite strong. To the east of the Hibernia Canyon, however, there is local weakening of the amplitude of the BTU reflection (Figure 4.4). Figure 4.5 is an amplitude extraction of the BTU reflection and there is a very clear North-South lination in the amplitude patterns. In particular, around the Hibernia P-15 bright spot is a local reduction in amplitude, with almost zero amplitude beneath the known small gas accumulations.

Figure 4.6 shows UA interpretation. M. Deptuck (pers. comm, 1998) has also mapped this reflection regionally using a 2 km x 2 km grid. Although this reflection is assumed to mark the top of the South Mara Unit, it is generally featureless within the area of interest. Reflection amplitude is generally moderate strength with little change.

4.3 South Mara Unit Stratigraphic Interpretation

Reflection amplitude within the South Mara is generally quite variable. Within the area of interest near the seismic bright spots, the reflection amplitude is generally weak.

Above and below the UA, reflections appear to converge in the updip direction. Truncation of reflections beneath the UA seems to indicate that the UA is an unconformity and that sediment flow direction is changing.

The South Mara Unit is generally low amplitude reflections onlapping against the BTU. Towards the basin center, the unit thickens, forming a wedge shape. Also towards the center of the basin, the South Mara grades into moderately continuous and low amplitude reflections.

From Table 3.2, matching the various characteristics of the observed seismic seems to indicate that the South Mara Unit, near and updip from the Hibernia P-15 bright spot, may represent “nearshore clastic sediments deposited by wave transport processes.” This is supported by the strike parallel trend in the bright spots (see section 4.5).

4.4 Gas Trapping Mechanism

From Figure 4.6, there is no obvious structural closure, nor faulting, of the UA to comprise a structural trap. For this reason, the trapping mechanism has to be a stratigraphic type trap. Since there is an unconformity immediately

overlying the bright spots, it is tempting to conclude that this trapping mechanism may be unconformity related. However, the bright spots do not terminate next to the unconformity so it is improbable that the stratigraphic trap is unconformity related. Examination of the bright spots in Figure 1.2, 4.7 and 4.8 seems to indicate that it is a related to paleogeomorphological features or pinchout.

4.5 Direct Hydrocarbon Indicators

Bright spots are the most prominent DHI present in the seismic data, and while they are correlated to dissolved gas at the Hibernia P-15 well, there are other mechanisms to create high amplitude anomalies. Having additional reasons to explain the presence of hydrocarbons improves the probability that hydrocarbons will be located there.

Figure 4.9 and Figure 4.10 shows the distribution of negative amplitude anomalies in relation to the BTU. The bright spots corresponding to the Hibernia P-15 accumulation is shown, strike parallel (perpendicular to the paleoslope). There are other bright spots to the northwest and southeast of the Hibernia P-15 bright spot that also strike parallel. To the northeast and east of the Hibernia P-15 bright spot are a number of other bright spots. These may, or may not be related to any dissolved gas.

Figures 4.7 and 4.8 shows the large bright spot to the east of the P-15 bright spot, and it is uncertain if that bright spot is a result of gas accumulation or not. Bright spots, by definition, are reflections caused by high impedance

contrasts. This would mean that immediately beneath the bright spot, there would be a local reduction in energy levels for other reflections. High amplitude anomalies which are caused by tuning effects, do not reduce the amount of downward energy. Since amplitude recovery methods do not accurately correct for these differences, a 'shadow zone' exists immediately below some bright spots, in particularly those with larger amounts of gas. Figure 4.5 shows that shadow zone beneath the P-15 and B-27 bright spots. This shadow zone is evident beneath the P-15 bright spot in Figures 1.1 and 1.2.

The large bright spot to the east of P-15 is ambiguous as to whether or not it is a bright spot or whether it is caused by tuning effects (see Figure 4.7). The amplitude anomaly occurs at an updip termination of a wedge of sediments. This is a situation where tuning could occur. Also note that towards the downdip part of the amplitude anomaly, below 1600 ms, there is no polarity reversal as expected (Figure 3.4). Tuning can result in higher amplitude anomalies but not necessarily an opposite polarity reflection. Of course, this is dependent upon the seismic wavelet; assuming that the wavelet stays the same throughout the survey, we would expect the same result here, but it is not evident throughout the brightspot. There is a polarity reversal in the updip part of the amplitude anomaly, near 1550 ms, but given the likelihood that the rest of the anomaly is caused by tuning, this may be the case here as well.

Other DHI's such as flat spots are not evident within this unit. This may be a result of the fact that the bright spots are caused by dissolved gas, so a gas/water contact would not necessarily develop.

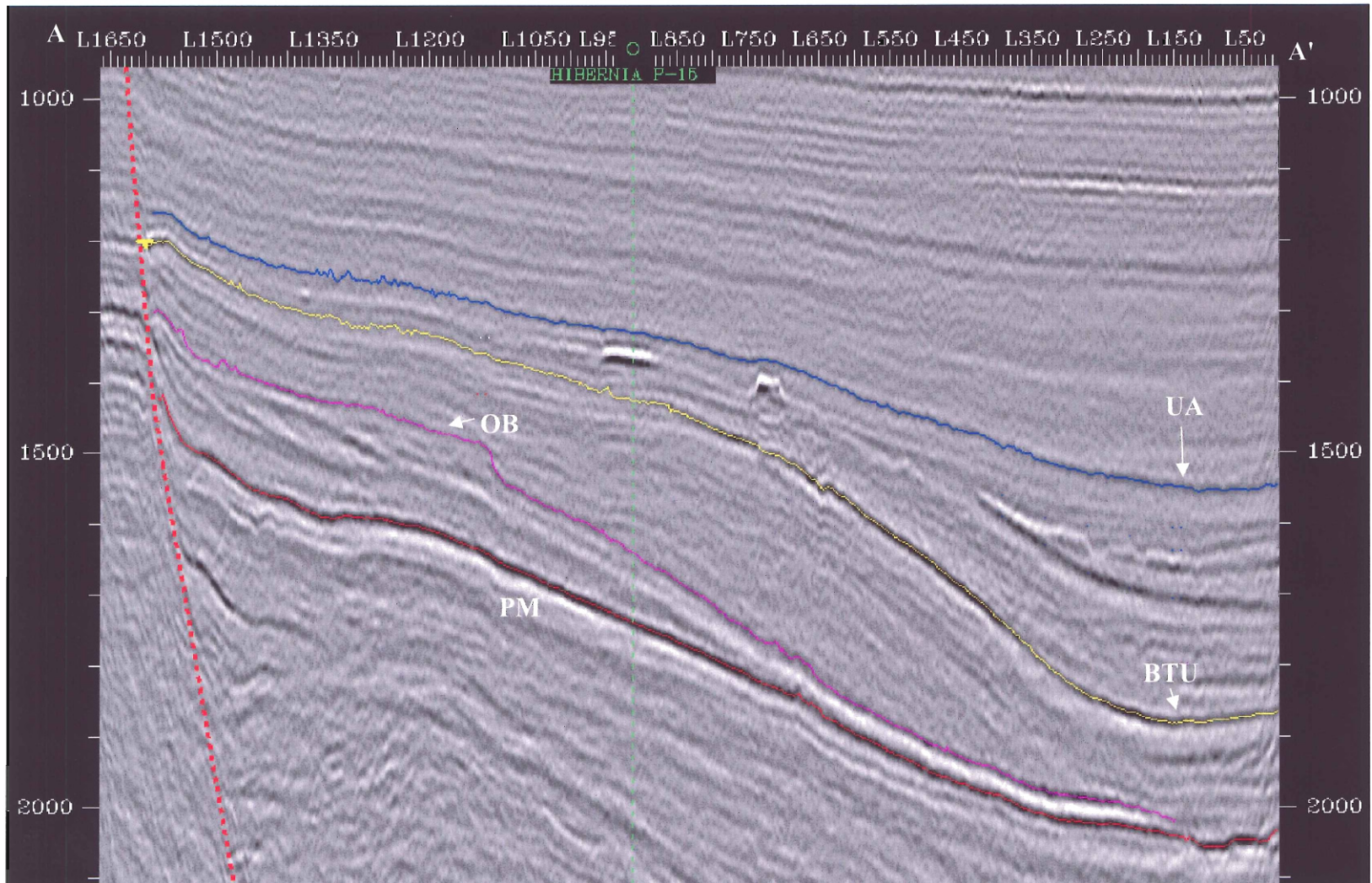


FIGURE 4.1 Seismic profile (same as Figure 1.1), illustrating the two main horizons interpreted. UA - 'Unconformity A', BTU - 'Base Tertiary Unconformity' reflection, OB - 'Top of the Otter Bay Member', 'PM' Petrel Member. Towards the right side of the profile, the OB and PM reflections converge (downdip). Tuning is evident here as the amplitude from the two reflections sum to create a higher amplitude composite reflection. (Trace 928 of Hibernia 3D survey.)

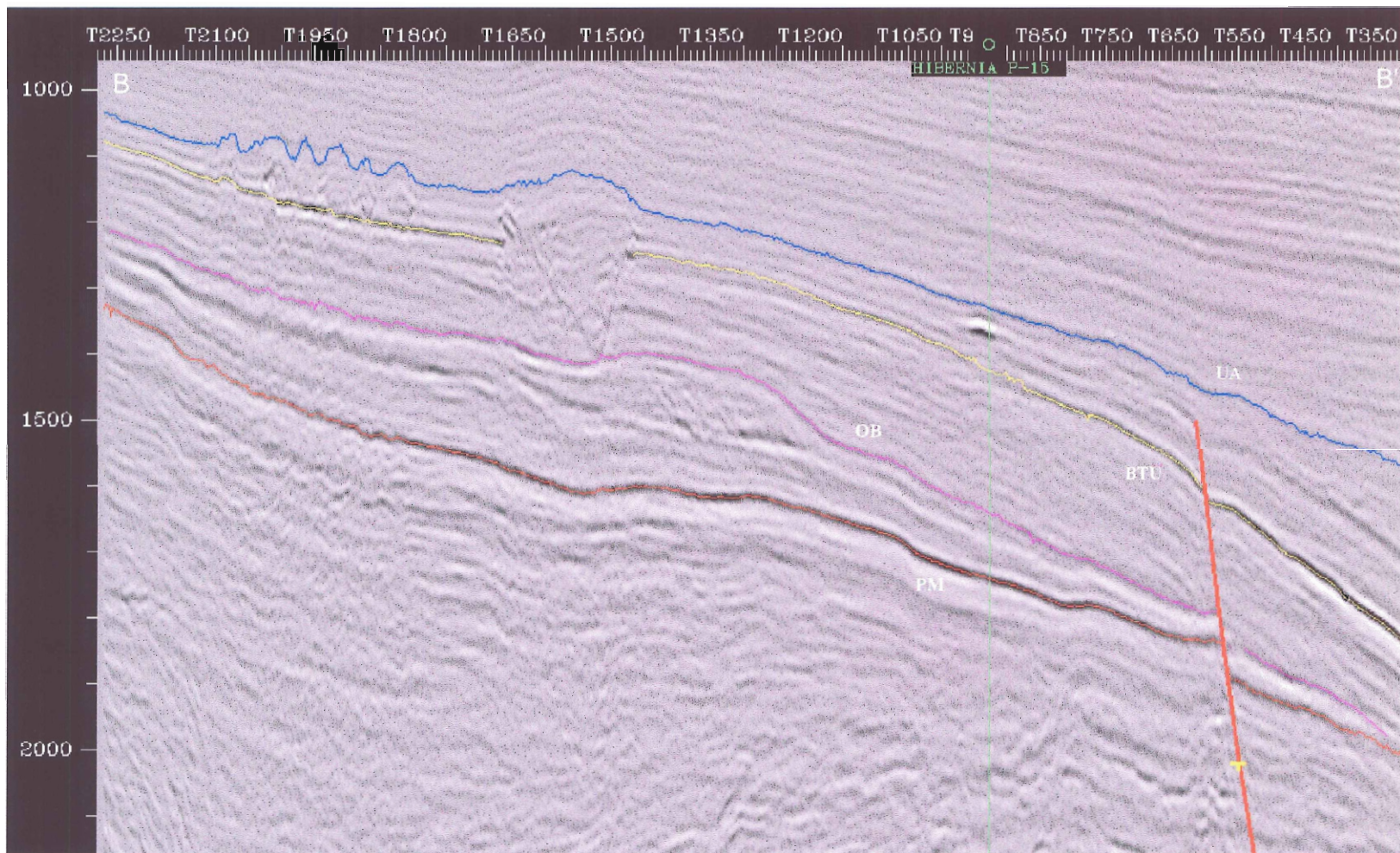


FIGURE 4.2 Seismic section showing two principal horizons. See Figure 4.1 for legend. (Line 912 of Hibernia 3D survey.)

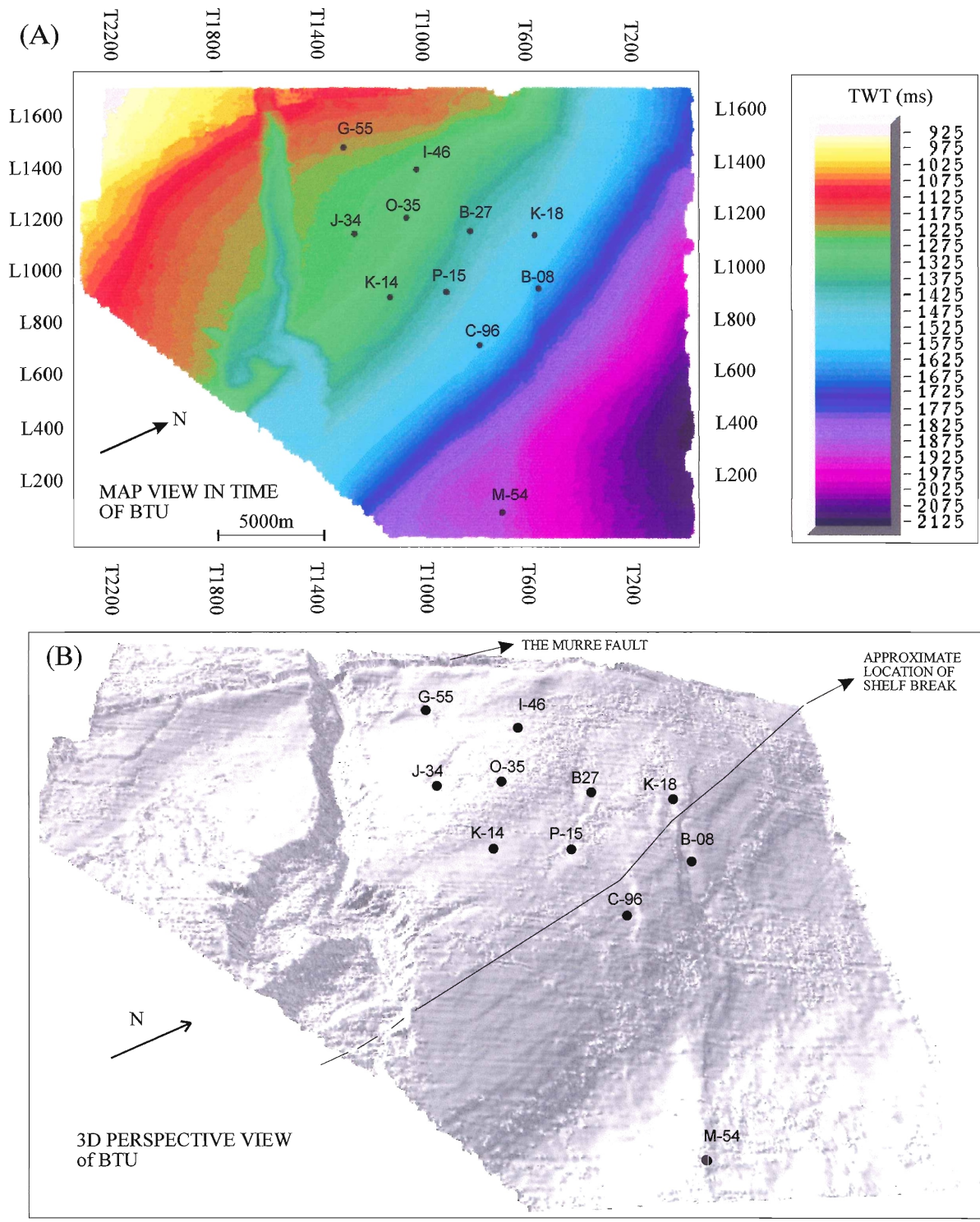


Figure 4.3 Interpretation of the BTU. The 3D perspective image reveals much more qualitative detail than the map view does. Note the Nautilus Fault is active after the BTU was formed. Modified after Friis (1997).

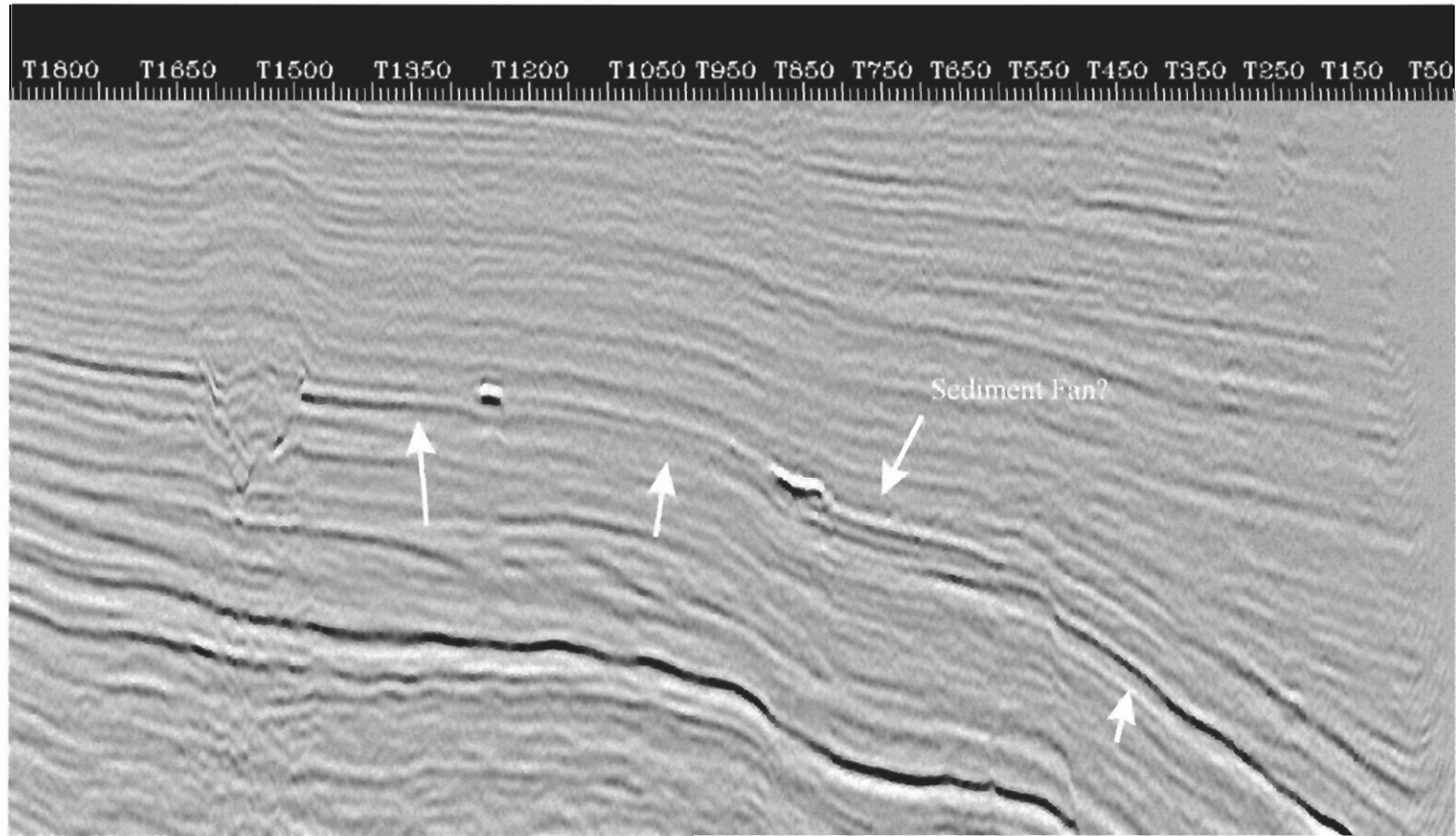


Figure 4.4 Seismic profile illustrating the weakening of the BTU reflection. The reflection is strong on the slope to the right of the diagram, and strong to the immediate right of the Hibernia Canyon. Between those two points, the amplitude decreases. This coincides with a relatively horizontal BTU erosion. Active erosion may have occurred and some sediment may have been deposited in the small local fan shown. Spatial trends of this reduction in amplitude is shown in Figure 4.5

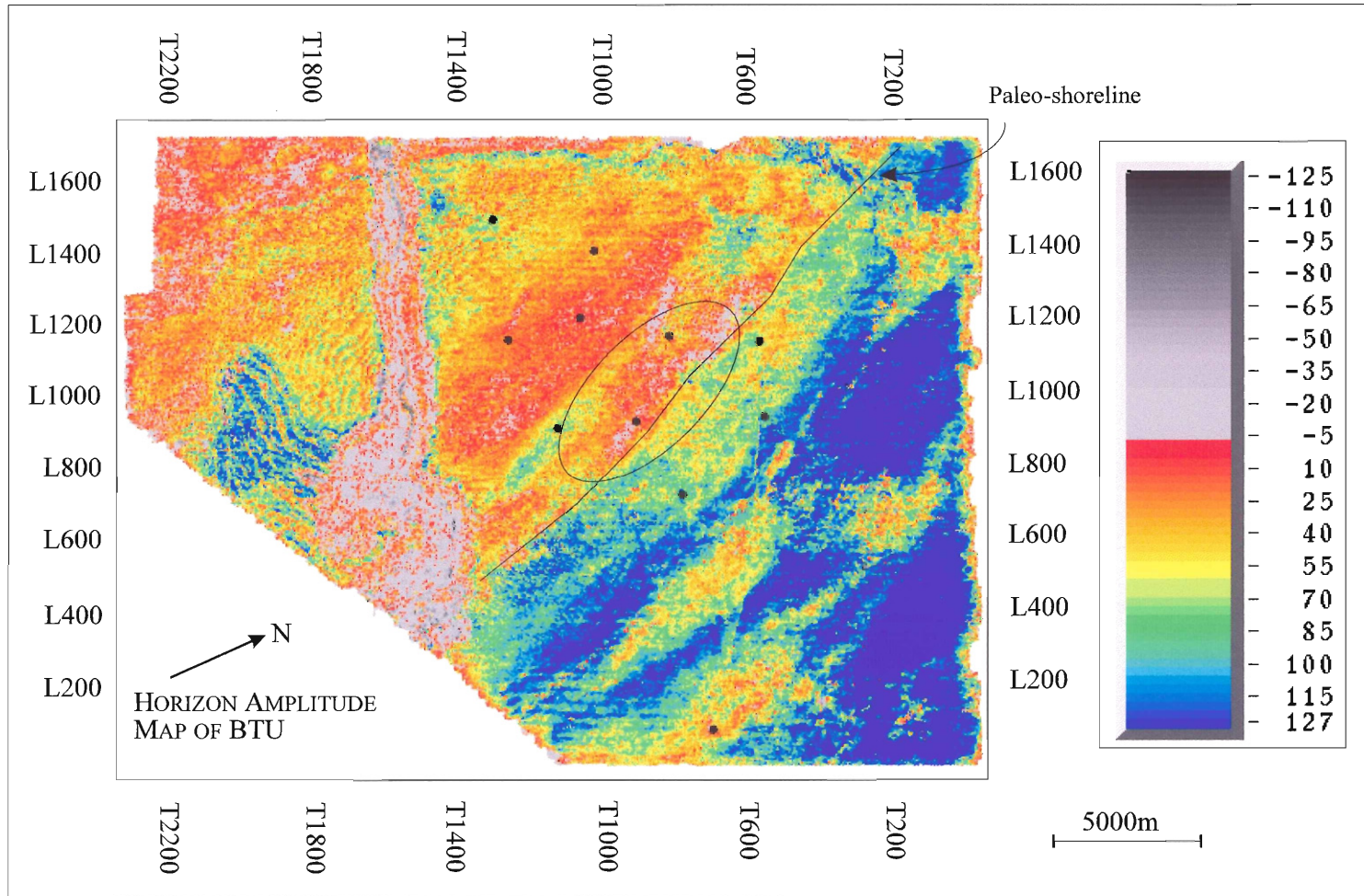


Figure 4.5 An amplitude extraction of the BTU reflection. There is a fairly well developed trend in the amplitudes. The trend appears to be predominantly North-South. Lower amplitudes are predominantly on the updip and flat part of the BTU. The paleo-shoreline is assumed to be parallel to the line drawn at the boundary between high and low amplitudes. Near the P-15 and B-27 wells (circled), there are pronounced low amplitudes in the horizon. These low amplitudes may be from the bright spots overlying the BTU in that area. See Figure 3.5 for an index of the wells.

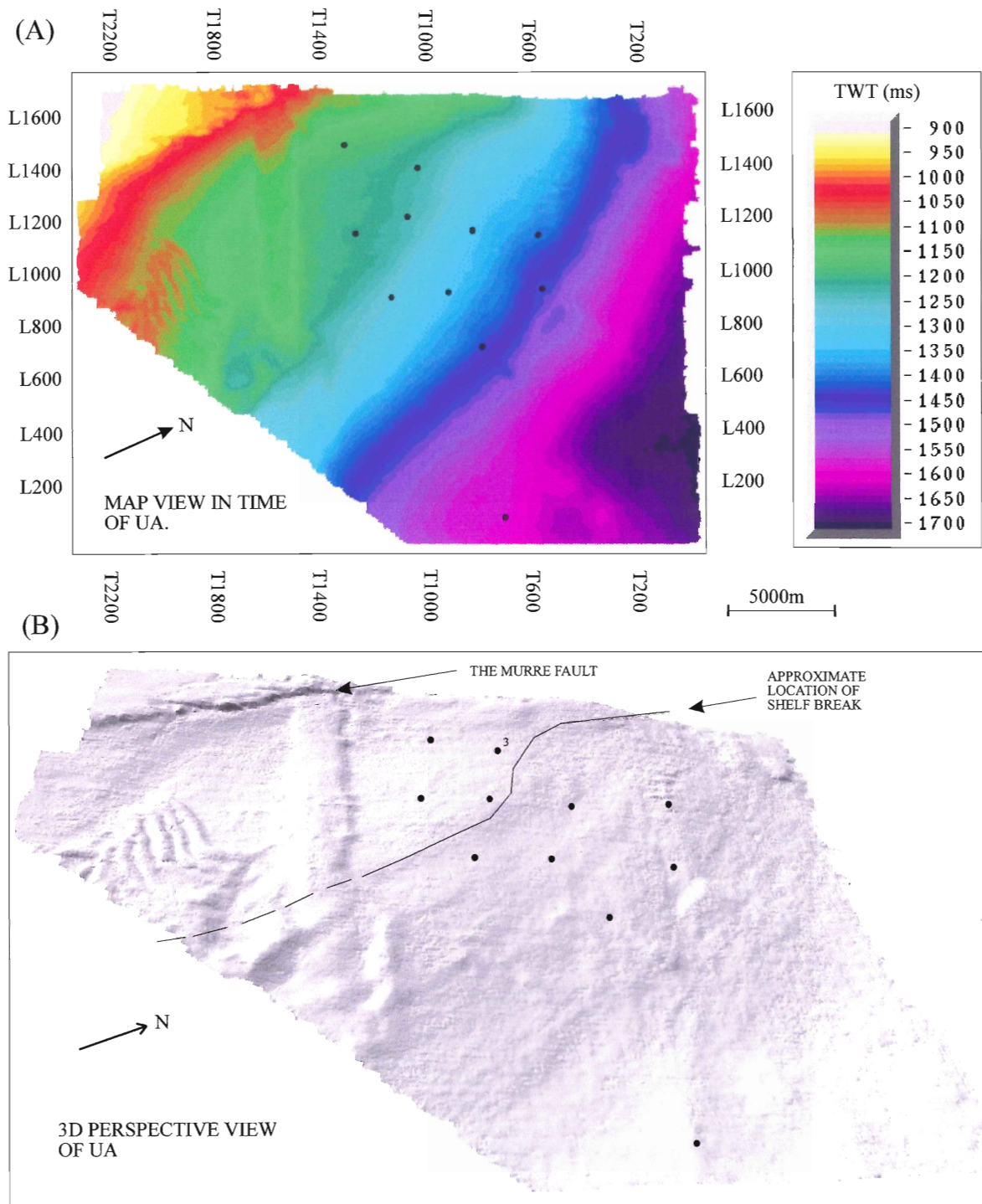


Figure 4.6 A map and a perspective view of the UA reflection. There is much less relief on this reflection surface than on the BTU reflection surface, with the exception of relief associated with the Hibernia Canyon (below T1400). Figure 2.5 has the legend for the wells. Modified from Friis (1997).

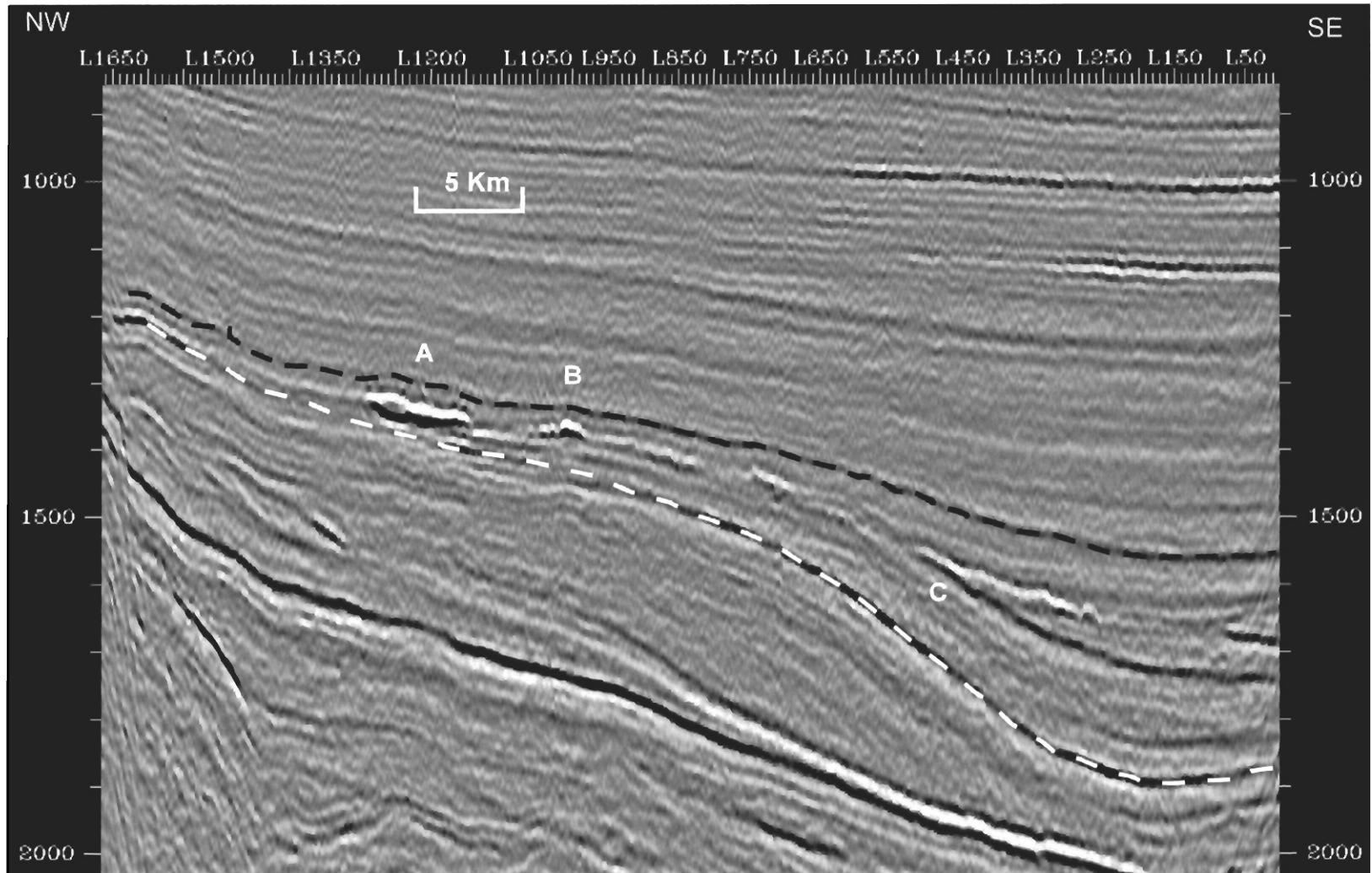


Figure 4.7 Two bright spots and a 3rd which may be an amplitude anomaly. 'A' is a bright spot to the west of B-27. 'B' is a bright spot to the east of B-27. 'C' is an amplitude anomaly which may be caused by tuning effects, or possibly dissolved gas as well. (Trace 850 of the 3D survey).

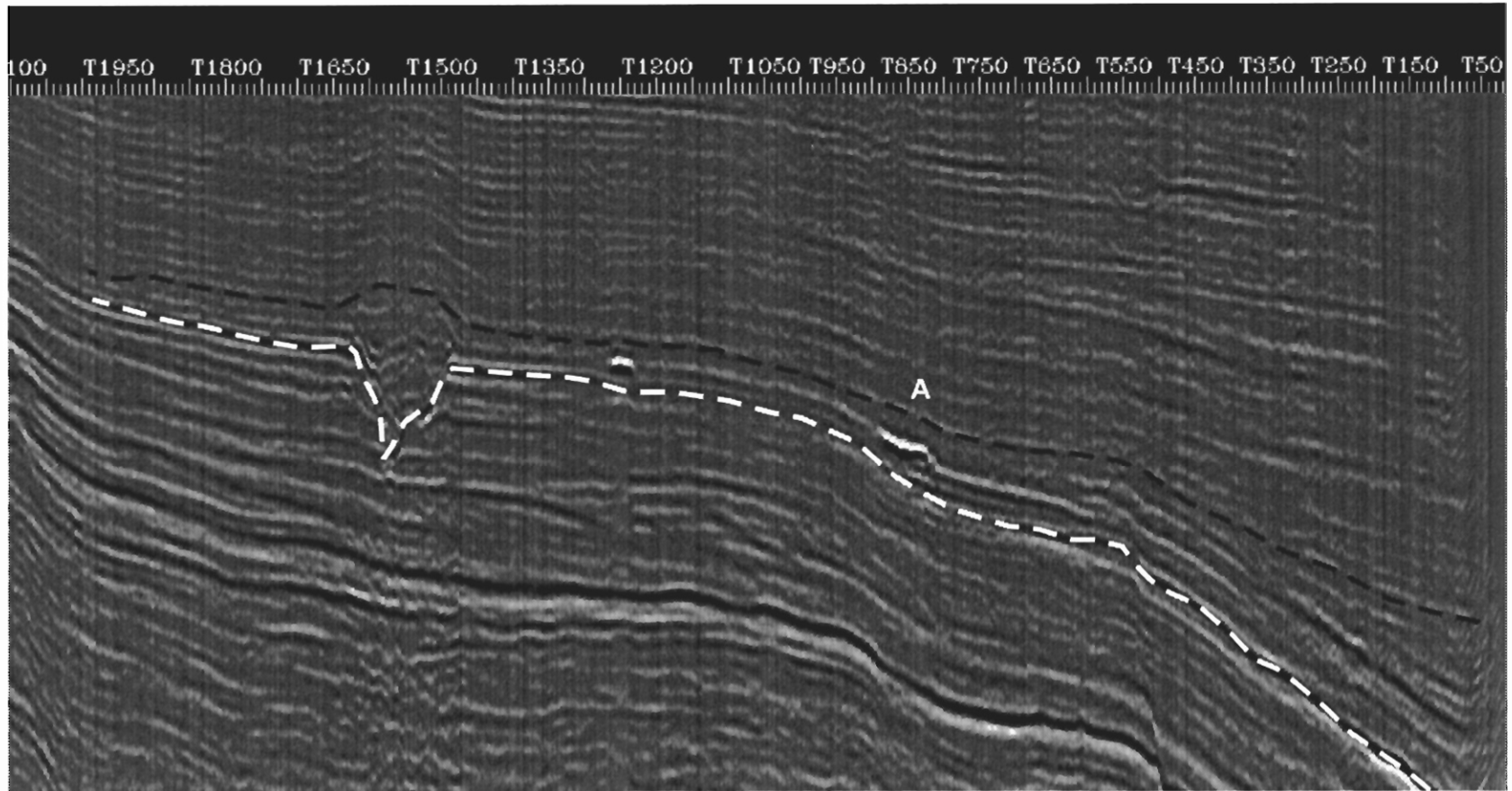


Figure 4.8 Image of bright near B-27 in a perpendicular direction from Figure 4.7. Bright spot geometry suggests that this bright spot may be a sediment fan. There is a lack of data near the edges due to lack of coverage or low data fold. The Nautilus fault is not marked but is present in this section. (Line 1188 of the data set.)

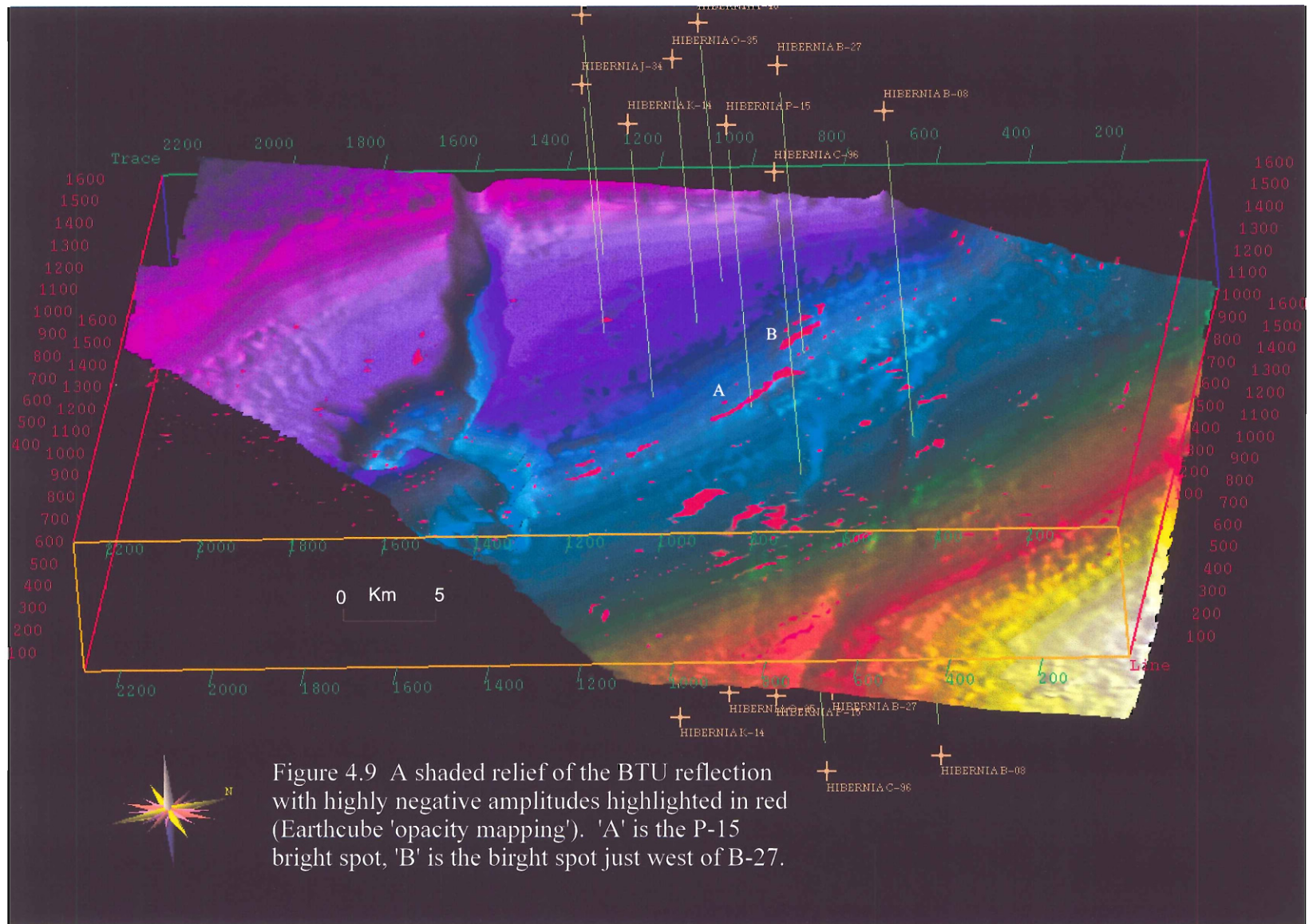
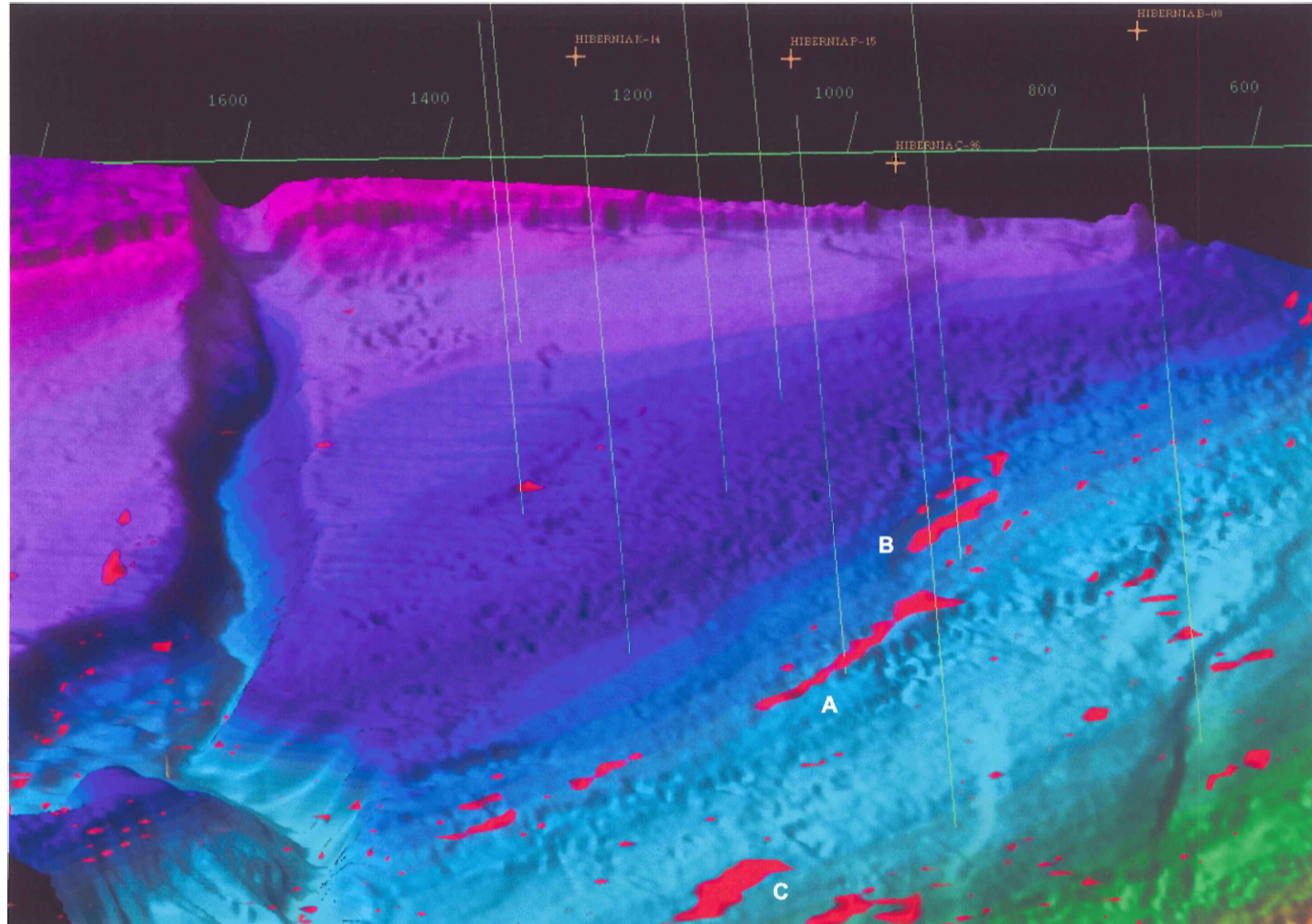


Figure 4.10
 Close-up image
 of Figure 4.9.
 Orientation is the
 same. Surface
 irregularities is
 readily apparent.
 Irregularities
 beneath bright
 spots may be due
 to noise or
 irregular
 sediment
 distribution in
 the South Mara
 Unit.



Legend: 'A' - P-15 bright spot; 'B' - bright spot to the west of B-27; 'C' - amplitude anomaly caused possibly by tuning. Scale is indicated by line counts; every 200 is 5 km.

5 *DISCUSSION*

Figure 4.10 indicates that probably not all of the bright spots in the Hibernia 3D survey are associated with dissolved gas. The simple geometry of the bright spot at the P-15 well does not reveal much in 2D profiles. With 3D data, the bright spot is sub-parallel to the paleo-shoreline/shelfbreak. This, along with the well developed trend of other bright spots following the same trend, is strongly supported by additional observations. Figures 4.7 and 4.8 shows what appears to be paleogeomorphologic features. Figure 4.4 seems to display what appears to be a sediment fan.

This idea was suggested by Sinclair et al. (1992), but they indicated that this trapping style could occur throughout the basin, indicating very little control. Sediment fans occur at all water depths. Figure 4.4 and 4.5 argues the case of shallow water depths. The reduction in the amplitude of the BTU reflection, as well as its very surprising distribution to 'plateau' areas (compare Figure 4.5 and 4.3) invites notions of wave induced erosion. The reduction in amplitude may be an indicator of reworked sediments. Reworking sediments may reduce the impedance contrast by mixing lithologies, making sharp lithological contacts more gradational by mixing.

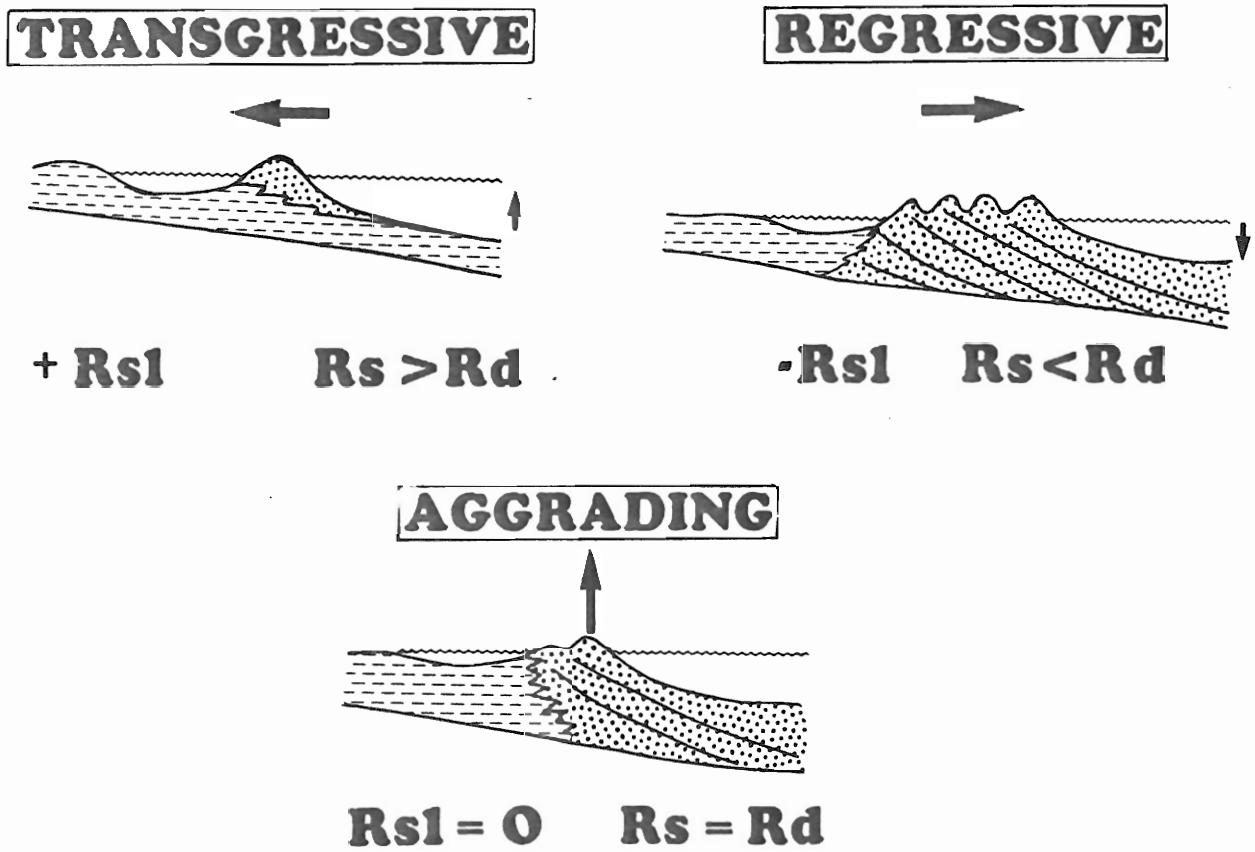
A partial story may be as follows (see Figure 2.1): an LST produces a South Mara sediment wedge in the central parts of the basin. This lowstand caused the BTU. A subsequent TST occurred very quickly and the paleo-shore

line may be just west of the P-15 well. The transition from a TST to a HST occurred slowly. As the wavebase rose, a small amount of erosion occurred and small sediment fans composed of reworked sediments were deposited parallel to the paleo-shoreline (Figure 5.1). These features were preserved shortly after by HST sediments.

This model has several unappealing implications. Chiefly, the Hibernia Canyon would not be a submarine canyon (Boyd, 1997) but have a terrestrial origin. The lack of terrestrial sediments may be removed or reworked by wave action. At the P-15 and J-34 wells, evidence exists for a shallower environment that submarine canyons typically do not form in. At the P-15 well, there exist nearshore indicators such as abundant glauconite and phosphatic grains (Friis, 1997). In addition, there are plentiful plant fragments and localized pyrite and siderite (Friis, 1997). Pyrite and siderite occur in reducing marine environments (Figure 5.2).

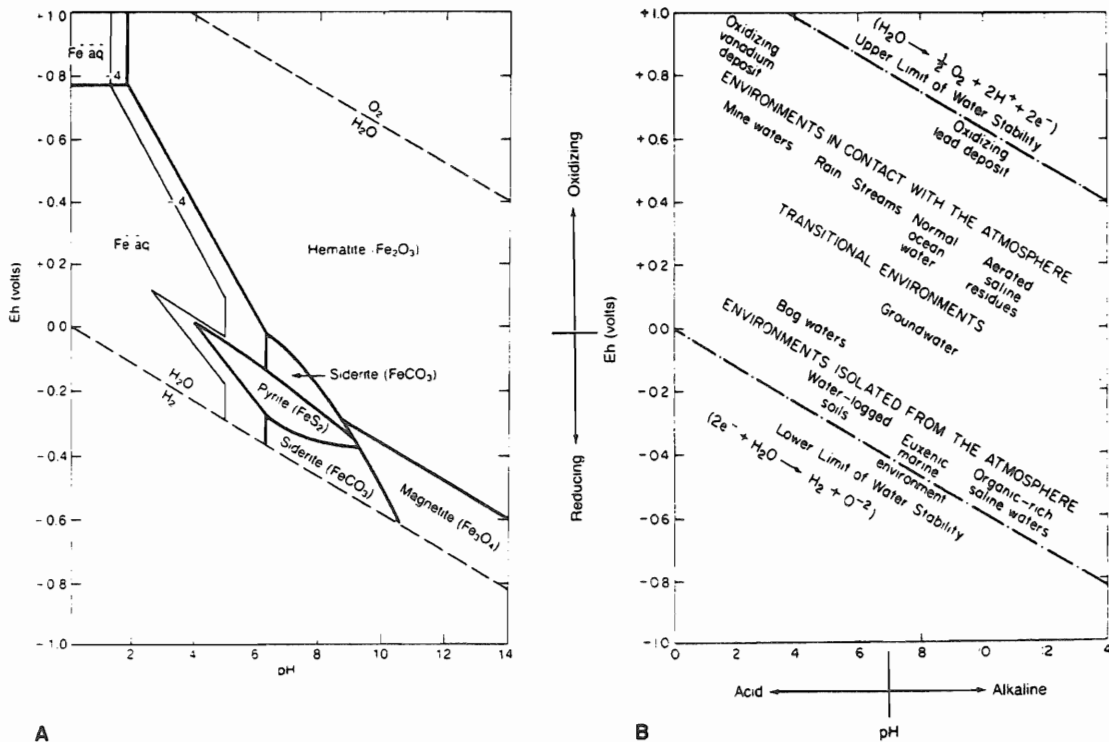
Finally, data to suggest that the sand units containing the P-15 and B-27 bright spots are near shore (and thus shallow) sediments are from the well data at P-15. Table 5.1 is a brief summary for paleoenvironmental estimation from well log data and seismic data. The P-15 bright spot contains plentiful phosphatic and glauconite, and forms lineations perpendicular to paleoslope. In addition, the base of the sands are fining upward sequences (see Figure 2.2), as indicated by the gamma ray logs. This suggests a beach or barrier bar sand deposited during a transgression.

Figure 5.1 Change in relative sea level and geometry of sand bars that may result. From Moslow (1984).



Stratigraphic models for clastic barrier shorelines as a function of the rate of sea level change (Rsl), rate of subsidence (R_s) and rate of deposition (R_d).

Figure 5.2 Iron geochemistry diagram to relate iron minerals to environment. From Boggs (1995).



A. Eh-pH diagram showing the stability fields of the common iron minerals, sulfides, and carbonates in water at 25°C and 1 atm total pressure. Total dissolved sulfur = 10^{-6} ; total dissolved carbonate = 10^{-6} . B. Graph showing Eh and pH of waters in some natural environments. (A. from Garrels, R. M., and C. L. Crist, 1965, *Solutions, minerals, and equilibria*. Fig. 7.21, p. 224, reprinted by permission of Harper & Row, New York. B. after Blatt, H., G. V. Middleton, and R. Murray, 1980, *Origin of sedimentary rocks*, 2nd ed. Fig. 6-12, p. 241, reprinted by permission of Prentice-Hall, Englewood Cliffs, N.J., based on data from Baas Becking, L. G. M. et al., 1960, Limits of the natural environment in terms of pH and oxidation-reduction potentials: *Jour. Geology*. v. 68, p. 243-284.)

Table 5.1 Summary of reservoir sandstone characteristics to their principal depositional environments.

Type of sand	Grain size or log profile	Typical grain size probability curve	Significant accessory minerals, etc	Dipmeter expression	Plan geometry and orientation	Primary porosity and permeability isotropy, etc
	m 25 Coarser Finer Gamma-ray - SP + 0	Phi scale 0 1 2 3 4 5		0° 10° 20° 30°		
AEOLIAN DUNE	up to 300 m	<p>98 % Coarser 2</p> <p>SUSPENSION SALTATION</p>	'Millet seed' frosted grains		SHEETS Downwind of source	Very good in dune foreset beds. Permeability restricted by fines in bottom sets. Permeability highest parallel with lamination
ALLUVIAL FAN	up to 3000 m	<p>Erratic, polymodal, and as braided</p>	Diverse unstable grains, micas	Depositional dips of 2 - 3° except narrow zone near mountains up to 30°. Individual sandstone units as braided	FANS thinning away from mountains. Coalescing to PRISMS parallel with mountain front.	Extremely variable, excellent to very poor depending on source material, climate, wind direction, etc
FLUVIATILE						
Braided		<p>SUSPENSION SALTATION TRACTION</p>	Diverse unstable grains, micas, carbonaceous. Shale intraclasts at base		RIBBONS, DENDROIDS, BELTS, parallel with palaeoslope. SHEETS	Variable, excellent to poor, inhomogeneous, lensing
Meandering		<p>TRACTION CHANNEL FLOOR POINT BAR TOP STRATUM TUM</p>	Mica, carbonaceous, especially in top stratum. Shale intraclasts at base		RIBBONS, DENDROIDS, BELTS parallel with palaeoslope. SHEETS	Channel deposits good but lensing and may be separated by tight top stratum or cemented layers
DELTAIC						
Distributary channel	NB upper reaches as fluvialite		Carbonaceous, micas		RIBBONS, DENDROIDS, parallel with palaeoslope	Good on axis but interdigitates with finer deposits on lateral margins
Distributary mouth bar			Carbonaceous, micas		PODS, perpendicular to palaeoslope, but prograde to form RIBBONS parallel with palaeoslope	Good, but deteriorates on margins. Top may be carbonate-cemented

6 CONCLUSIONS

Seismic methods show that there are many amplitude anomalies at Hibernia. However, since there is more than one way to generate amplitude anomalies, not all of these anomalies are 'bright spots', which are indicative of gas accumulations. One of the other prevailing ways to generate an amplitude anomaly is through tuning effects, which is caused by constructive interference between two reflections. Bright spots, on the other hand, are a result of much stronger than average impedance contrasts so the reflection from them is much greater.

The differences between these two can barely be detected seismically due to their small size: the real bright spot at P-15 appears to have a small shadow zone beneath them as a result of the high impedance contrast. Tuning effects may produce the same polarity reversal when the reflectors are at specific separations.

A more useful tool is paleo-environmental interpretation using existing sand models. The sands in DST #12 at the Hibernia P-15 well seem to be deposited near the shoreline and shore-parallel. This strongly suggests that the sands are a buried beach or barrier bar, encased in shale during a 'jump' in RSL. Other bright spots within the South Mara Unit may also contain gas, but there is compelling evidence for many of the bright spots to at least be the partial result of tuning effects.

7 REFERENCES AND BIBLIOGRAPHY

- Amery, G. B., 1993. Basics of seismic velocities. *In* The Leading Edge. Society of Exploration Geophysicists (Nov 1993, pages 1087-1091)
- Boggs, Sam, 1995. Principles of Sedimentology and Stratigraphy. 2nd Ed. Englewood Cliffs, N.J.: Prentice Hall.
- Boyd, H.K., 1997. Modelling of a Paleocene canyon to determine lithologic fill. B.Sc. Thesis, Dept. of Earth Sciences, Dalhousie University. Pp. 1-31
- Brown, A.R., 1996. AAPG Memoir 42: Interpretation of 3D seismic.
- Desroches, K.J., 1992. A subsidence, compaction, pressure, temperature and maturity history of the Hibernia B-08 well, Grand Banks, Newfoundland. B.Sc Thesis, Dept. of Earth Sciences, Dalhousie University. Pp. 1-8.
- Driscoll, N.W., J.R. Hogg, N. Christie-Blick and G.D. Karner, 1995. Extensional tectonics in the Jeanne d'Arc basin: Implications for the timing of break-up between Grand Banks and Iberia. *In* The tectonics, sedimentation, and palaeoceanography of the North Atlantic region. *Edited by* R.A. Scrutton, M.S. Stoker, G.B. Shimmiel and A.W. Tudhope. Geological Society of London. Special Publication 90, pp. 1-28.
- Friis, N., 1997. A well log and 3-D seismic study of the Late Cretaceous to Eocene deposits in the Hibernia area of the Jeanne d'Arc Basin, offshore Newfoundland, Canada. Dept. of Earth Sciences, University of Aarhus, M.Sc thesis.
- Grant, A.C., McAlpine, K.D., and Wade, J.A., 1986. The continental margin of

eastern Canada: geological framework and petroleum potential. *In*: Future Petroleum provinces of the world. Halbouty, M.T. (Ed). AAPG Memoir 40: 177-205.

Kallweit, R. S., and Wood, L. C., 1982. The limits of resolution of zero-phase wavelets. *In* Geophysics. Society of Exploration Geophysicists. **47**: 7. Pp. 1035-1046.

Kearney, P. and Brooks, M., 1984. An Introduction to Geophysical Exploration. *2nd Ed.* Blackwell Scientific Publications. Pp. 8-20.

Lindsey, J. P., 1989. The Fresnel Zone and its interpretive significance *in* Seismic Interpretation: 18 *In* Geophysics: The Leading Edge of Exploration. Society of Exploration Geophysicists. October 1989 pages 33-39

McAlpine, K.D., 1990. Mesozoic stratigraphy, sedimentary evolution, and petroleum potential of the Jeanne d'Arc Basin, Grand Banks of Newfoundland. Geological Survey of Canada Paper 89-17, pp. 1-17, 41-47.

McAlpine, K.D., 1990b. GSC Open file #2201.

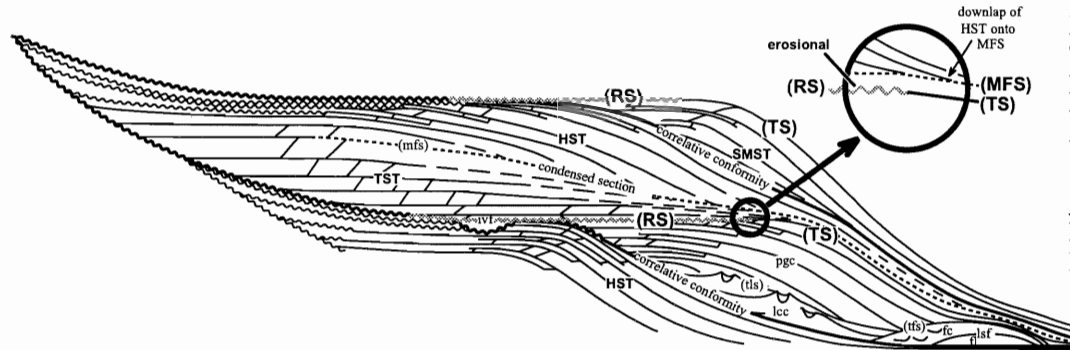
Meckel, L. D., and Nath, A. K., 1977. Geologic considerations for Stratigraphic Modeling and Interpretation. *In* Geophysics. Society of Exploration Geophysicists. (volume? Issue?) Pp. 417-438.

Robertson, J. D., and Nogami, H. H., 1984. Complex seismic trace analysis of thin beds. *In* Geophysics. Society of Exploration Geophysicists **49**: 4 Pp. 344-352.

Sangree, J.B., and Widmier, J. M., 1977. Seismic Stratigraphy and Global Changes of Sea Level, Part 9: Seismic Interpretation of Clastic Depositional Facies. *In*

- AAPG Memoir 26: Seismic Stratigraphy –Applications to hydrocarbon exploration. AAPG Press.
- Schlumberger, 1987. Log Interpretation Principles/Applications. Schlumberger Educational Services.
- Sinclair, I. K., McAlpine K.D. et al., 1992. Petroleum resources of the Jeanne d’Arc Basin and environs, Grand Banks, Newfoundland. Geological Survey of Canada Paper 92-8, pp. 1-45.
- Tankard, A.J., and Welsink, H.J., 1987. Extensional tectonics and stratigraphy of the Hibernia Oilfield, Grand Banks, Newfoundland. AAPG Bulletin **71**:1445-1466.
- Telford, W.M., Geldart, L.P., and Sheriff, R.E., 1990. Applied Geophysics, *2nd Ed.* Press Syndicate of the Univ. of Cambridge. Pp.262-264.
- Wade, J. A., Brown, D. E., Traverse, A., and Fensome, R. A., 1996. The Triassic-Jurassic Fundy Basin, eastern Canada: regional setting, stratigraphy and hydrocarbon potential *In Atlantic Geology Edited by Pickerill, R. K., Barr, S. M., and Williams, G. L. v. 32*: 189-206.
- Yilmaz, Ozdogan, 1987. Seismic Data Processing. SEG Press.

A) IN DEPTH



The principal conceptual model for sequence interpretation from Friis (1997).

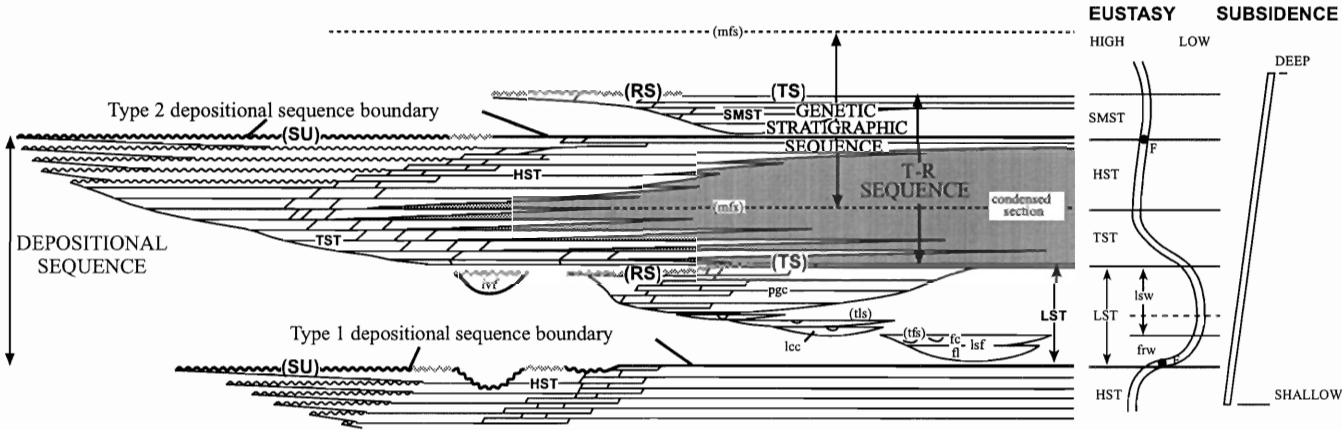
Surfaces

- SU= subaerial unconformity
- MFS= maximum flooding surface
- TLS= top lowstand surface
- RS= Ravinement Surface
- tsfs= top slope fan surface
- tbfs= top basin floor fan surface

Systems Tracts

- HST= high stand systems tract
- LST= lowstand systems tract (sometimes divided into)
 - lsw= lowstand wedge
 - ivf= incised valley fill
 - pgc= prograding complex
 - sf= lowstand slope fan
 - frw= forced regressive wedge
 - bf= lowstand basin floor fan
 - frw= forced regressive wedge
- TST= transgressive systems tract
- SMST= shelf margin systems tract

B) IN GEOLOGIC TIME



C)

